AD-A124 736 A CRYOGENIC ARGON IONIZATION CHAMBER DETECTOR FOR ANALYSIS OF RADIOACTIVE..(U) AIR FORCE INST OF TECH WRIGHT-PATTERSON AFB OH SCHOOL OF ENGI.. S R BERGGREN 1/1

UNCLASSIFIED MAR 82 AFIT/GNE/PH/82-3 F/G 18/2 NL

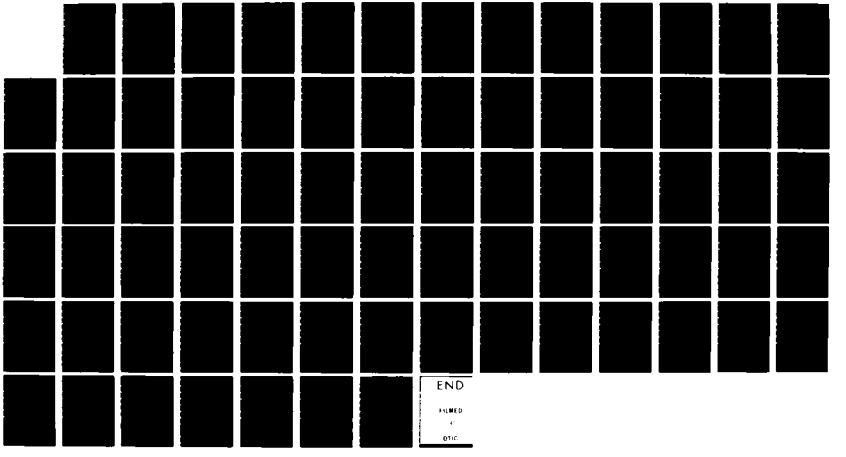

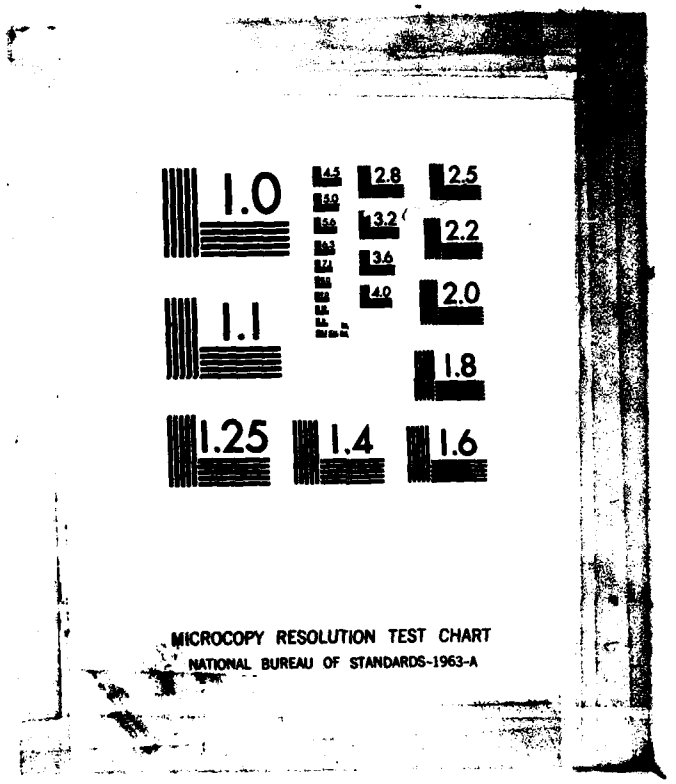
1.0
1.1
1.25
1.4
1.6
2.8
3.2
3.6
4.0
2.5
2.2
2.0
1.8
MICROCOPY RESOLUTION TEST CHART
NATIONAL BUREAU OF STANDARDS-1963-A

A CRYOGENIC ARGON IONIZATION CHAMBER DETECTOR FOR ANALYSIS OF RADIOACTIVE NOBLE GASES

THESIS

AFIT/GNE/PH/82-3

Stephen Ralph Berggren
Capt USAF

Approved for public release; distribution unlimited

AFIT/GNE/PH/82-3

A CRYOGENIC ARGON IONIZATION CHAMBER DETECTOR FOR ANALYSIS OF RADIOACTIVE NOBLE GASES

THESIS

Presented to the Faculty of the School of Engineering

of the Air Force Institute of Technology

Air University

in Partial Fulfillment of the

Requirements for the Degree of

Master of Science

by

Stephen R. Berggren, B.S.

Capt. USAF

Graduate Nuclear Engineering

March 1982

Approved for public release; distribution unlimited.

Preface

This thesis is the result of a suggestion that a liquid argon detector might prove to be a better means of analyzing radioactive xenon. The original goal was to determine if this were true. As it turned out, the design, construction and testing of an argon detector was a very interesting and complex subject in itself. Thus, the report concerns itself more with the theory, design, operation and characteristics of a cryogenic (liquid or solid) argon detector. The link to xenon was not entirely lost, however. The detector design was optimized to work with small noble gas samples, particularly xenon. I hope that what I have done will be built upon by others so that the original goal of the thesis will eventually be realized. To those who may follow, good luck.

This thesis was not entirely my own work. Claude Brassard's article 'Liquid Ionization Detectors' and his list of references were a superb starting point. My advisor, Dr. George John contributed enormously to the design and testing of the detector and guided the entire effort. The personnel of the School Shop and Jim Ray, the glassblower, turned my design fantasies into working hardware. I thank them all.

Contents

List of Figures

List of Tables

Abstract

Two ionization chamber detectors, using liquid or solid argon as their medium were designed, constructed and tested as an improved means of analyzing quantitatively xenon 131m and xenon 133. Problems with the first detector, including vibrational noise and inadequate temperature control, limited its use to studies using solid argon. In the second design, many operating problems of the first detector were corrected.

Properties of the detectors were studied using external gamma sources and xenon 131m dispersed inside the detector medium. The xenon sample and argon were purified and cryogenically pumped into the detector for spectral analysis. Electric field strengths used were from 100 to 900 kV/m. Both the purity of the argon and bias voltages affected resolution by changing the trapping distance of the electrons in the medium. Lower temperatures increased detection efficiency by condensing more of the sample into the cell.

No clearly recognizable energy peak could be found in spectra from external or internal sources. This is attributed to impurities in the argon medium, to positive ion trapping in the flaws of the crystals and to var tion in pulse height with the radial position of interaction in the medium. Detection efficiency for an internal xenon source is less than 10 percent. This is attributed to impurities or to the trapping of the xenon sample outside of the cell. Accurate evaluation of the capabilities of this type of detector cannot be made until the xenon sample can be reliably moved to the detector, the argon purity improved and the design modified to eliminate the position dependence of the signals.

A CRYOGENIC ARGON IONIZATION CHAMBER DETECTOR FOR ANALYSIS OF RADIOACTIVE NOBLE GASES

I. INTRODUCTION

Subject

The subject of this thesis is the design, construction and testing of an ionization chamber using liquid or solid argon as the detector medium and its application to the quantitative analysis of radionuclides of noble gases. The theory on which such detectors are based and the work of other researchers suggest that this detector offers potential advantages in both resolution and detection geometry over the current methods of analysis. The detector may be a more accurate means of analyzing quantitatively mixtures of Xe 131m and Xe 133 than the methods currently used.

Background

Several subjects are presented as background information on cryogenic argon detectors and on xenon and its analysis. First, the sources of xenon and the reasons for analyzing it are discussed. The decay schemes of the two most important xenon radionuclides are presented. Then, a comparison is made between the advantages of two current methods of xenon analysis and the theoretical advantages of analysis by a cryogenic argon detector. Finally, some data on argon, xenon and nitrogen are presented as background for the design criteria.

Several noble gas radionuclides are products of nuclear fission. They are contained in effluent gases from reactors and reactor fuel processing plants. As such they are potential environmental pollutants. Thus, it is important to measure accurately their concentration in air samples.

Of the noble gases, xenon was selected for analysis because of its physical and nuclear properties. Its freezing point, slightly higher than argon, makes it easy to handle and introduce into a cryogenic detector. It also allows the xenon to be easily recovered from the argon medium by distillation. The decay schemes of xenon radionuclides are also suitable. Of the many xenon fission products, only Xe 131m and Xe 133 have half lives long enough to be usable. Their half lives are 11.92 days and 5.25 days, respectively (Ref 15). Figures 1 and 2 show the decay schemes of the two nuclides. Tables 1 and 2 contain the energies and relative abundance of the two nuclides' most common emissions (Ref 13, 18). The electron emissions of Xe 131m and Xe 133 should be efficiently detected. The x-rays at about 30 keV should also be seen. The monoenergetic internal conversion electron of Xe 131m should also be ideal for energy calibration and resolution analysis.

A current method of quantitative analysis of xenon uses a scintillation counter (Ref 12). Toluene, with a fluorescing material added, is used as the scintillating medium with the xenon sample dissolved in it. This method virtually eliminates self-absorption and geometric losses, giving essentially 100 percent efficiency in detecting electrons. The main drawbacks to the use of scintillation counters for xenon analysis are their low efficiency in detecting photons and their poor energy resolution (Ref 14).

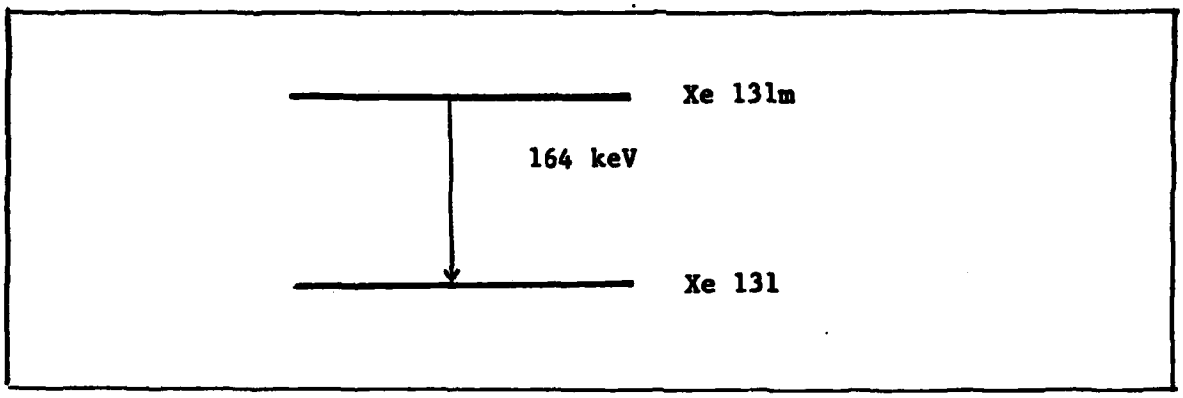

Figure 1. Decay Diagram of Xe 131m (15)

Table 1. Decay Emissions of Xe 131m (15)

Type	Energy (keV)	Abundance (per Xe 131m decay)
Gamma	163.98	0.022
K IC electrons	129.4	0.633
L,M IC electrons	158.5 -162.9	0.405
K x-rays	29.5 - 34.4	0.550
Auger electron	23.70- 25.0	0.083

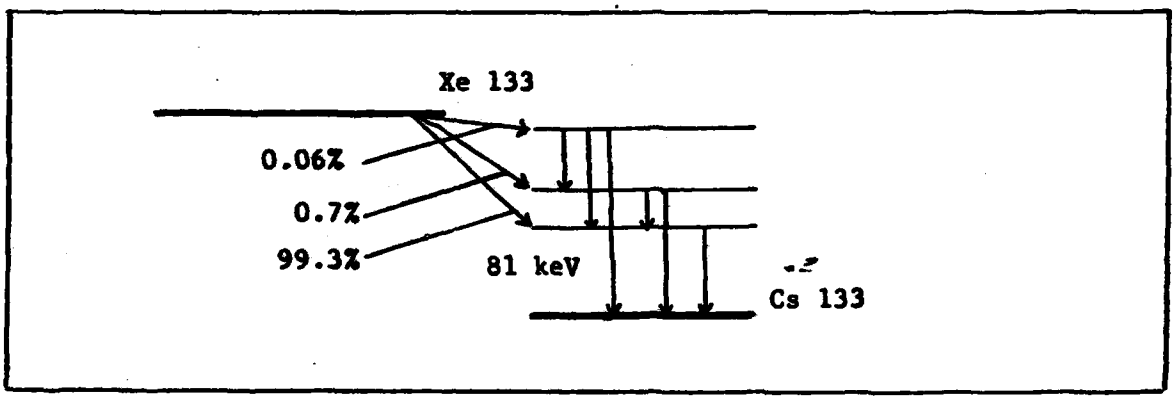

Figure 2. Decay Diagram of Xe 133 (15)

Table 2. Decay Emissions of Xe 133 (15)

Type	Energy (keV)	Abundance (per Xe 133 decay)
Beta	346	0.993
Gamma	81.0	0.378
K IC electrons	45.0	0.527
L IC electrons	75.0 - 76.0	0.089
K x-rays	30.6 - 35.8	0.464
Auger electrons	25	0.063

An alternate method for analyzing xenon is currently under investigation (Ref 13, 14). In this method, the xenon is solidified onto a thin beryllium window and detected using semiconductor detectors. The semiconductor detectors give much better resolution of x-ray and gamma-ray energies than the scintillation detector. However, the use of a beryllium window and the position and thickness of the solidified xenon create window absorption, detection geometry and self-absorption problems not found in scintillation detection.

The cryogenic argon detector can offer the detection efficiencies of the scintillation detector and resolution comparable to that of the semiconductor detector. The combination of good efficiency and good resolution would make the argon detector superior to scintillation or semiconductor detectors for xenon analysis.

As with the scintillation detector, the xenon sample is mixed into the argon detector's medium. This eliminates absorption and geometry problems. Further, the argon detector's efficiency in detecting betas and conversion electrons should be slightly better than that of the scintillation counter because of reduced edge effects. A 160 keV electron travels about 0.032 cm in liquid argon and about 0.036 cm in toluene. X-ray efficiency should also be better for the argon detector. The linear attenuation coefficient for all interactions for a 30 keV photon is 3.9 cm^{-1} in liquid argon and 0.23 cm^{-1} in toluene.

The theoretical energy resolution of cryogenic argon detectors can be much better than that of scintillation counters and can approach that of semiconductor detectors (Ref 1). The contribution of the

detector to the full width at half maximum (FWHM) of a peak in a pulse-height spectrum can be expressed as:

$$\text{FWHM Detector} = 2.35\sqrt{EwF}$$

where E is the energy of the emissions corresponding to the peak, w is the average energy required for the creation of one electron-ion pair and F is the Fano factor. Table 3 contains a comparison of the FWHM contributions of three detectors: a scintillation detector, a lithium-drifted silicon semiconductor detector and a liquid argon detector. The Fano factor listed in the table for liquid argon was not measured experimentally but was calculated from theory (Ref 3). Although the argon detector's theoretical resolution has not yet been approached experimentally, improvement by a factor of eight over the resolution of a scintillation detector can be expected.

Table 3. Comparison of Detector Contribution to Resolution

Detector	w (eV/ion pair)	Fano Factor	FWHM at 160 keV (keV)
Scintillation	179 *	1.00 (Ref 13)	12.58
Silicon	3.62 (Ref 14)	0.084 (Ref 13)	0.52
Liquid Argon	23.6 (Ref 20)	0.107 (Ref 3)	1.49

* 1/(0.056 e^- per light eV * 0.10 fluorescence efficiency) (Ref 17)

Table 4 gives miscellaneous physical data about xenon, argon and nitrogen. This data is used to establish criteria for the design of the detectors.

Scope and Organization

Presented in this report are the designs, operating characteristic and results obtained from two different cryogenic argon detector cells. The design requirements for the first detector were dictated by the

Table 4. Properties of Xenon, Argon and Nitrogen (Ref 10)

Property	Element Xenon	Argon	Nitrogen
Atomic number	54	18	7
Atomic weight (Avg.)	131.3	39.9	14.0
Boiling point (C)	-107.1	-185.7	-195.8
Melting point (C)	-112	-189.2	-209.86
Liquid density (g/ml)	3.52 (-109C)	1.40 (-186C)	0.808 (-195.8C)
Solid density (g/ml	2.70 (-140C)	1.65 (-233C)	1.026 (-252.5C)
Vapor pressure (torr)	0 (-195C)	196 (-195C)	760 (-195C)

intended application as well as the theory of liquid argon detectors. Additional requirements came from a study of the detector designs used by other experimenters. The resulting characteristics of the detector are discussed. The characteristics include the effects of impurities, biasing voltage, and temperature on the spectra obtained from xenon 131m and an external gamma source. Because of vibration and temperature control problems, the first detector was used only to study solid argon as a detector medium. Most of the design deficiencies of the first detector were corrected in the design of the second. The second detector was used for a limited study of liquid argon as a detector medium. Some results from the second detector are presented and several suggestions on improving its performance are made.

The report is organized in the following manner. The theory of cryogenic argon detectors is presented in section II. Section III is a description of the design criteria used. The design and construction of the two detectors and the gas handling system (GHS) is also presented. Section IV contains the operating procedures, the characteristics of each system and the results obtained. Finally, the discussion, conclusions and recommendations for further work are presented in section V.

II. THEORY

Ionization Chambers

Cryogenic argon ionization chamber detectors operate on the same basic principles as other ionization detectors and have similar characteristics. The characteristics which are most desirable in a detector used for analysis by pulse-height spectrometry are high resolution and high efficiency. High resolution results from efficient conversion of radiation energy to electron-ion pairs, rapid and efficient collection of the resulting charges, low statistical variation in the number of ion pairs produced, and a linear relationship between the ion pairs produced and the pulse detected. Detection efficiency results when all or most of the radiation from the source interacts in the detection medium.

Detection Efficiency

Detection efficiency is determined by the fraction of the decay events occuring in the source that are recorded by the detector. When the source is dispersed in the detection medium, as in the liquid scintillator and cryogenic argon detector, there are almost no losses due to geometry factors. The only losses occur when radiation from an event escapes the detector without interacting with the medium or deposits so little energy before escaping that the resulting charges cannot be detected. This occurs only at the surface of the detector volume. When the detector's dimensions are significantly larger than

the range of the radiation in the medium, these losses are negligible and the detection efficiency is approximately 1.0. The argon detectors designed have a radius of 0.5 cm compared to a 160 keV electron's path length of 0.032 cm and a 30 keV photon's mean free path of 0.26 cm. Thus the detectors can be expected to have a detection efficiency of about 1.0.

Charge Production

The energy deposited by the radiation in the detector medium creates electron-ion pairs. For a given amount of energy deposited, the number of ion pairs created depends on the average amount of energy required to produce one pair. If the average energy required is small, more ion pairs are created, giving a larger signal and reducing the statistical variation in the pulse height.

The average amount of energy required to produce an electron-ion pair, w, is determined by the composition and state of the medium. For pure liquid argon, w is 23.6 (+0.5, -0.3) eV per ion pair, (Ref 20) while for argon gas it is 27.0 (Ref 14). For solid argon it is unknown but is assumed to be approximately the same as for the liquid. For liquid xenon, w is 16.5. When 1.6 percent xenon is dissolved into liquid argon, ionization is enhanced by 13 percent, resulting in a smaller value for w (Ref 19).

Charge Collection

The electrons and positive ions produced in the medium drift in the applied electric field and are collected on the anode and cathode, respectively. Their drift produces the electric pulse detected by the preamplifier. The rate of their drift determines the rise time of the

pulse while the distance they drift determines the pulse height. Ideally, both the electrons and ions should drift as rapidly as possible and without interference from impurities or recombination.

Electron and Ion Drift Velocities. The electron drift velocity in liquid argon as a function of the applied field is shown in figure 3. Note that the impurities increase the drift velocity. This effect is believed to occur because "inelastic scattering of impurity atoms provide a more efficient means of energy loss and hence cool the electrons down" (Ref 8).

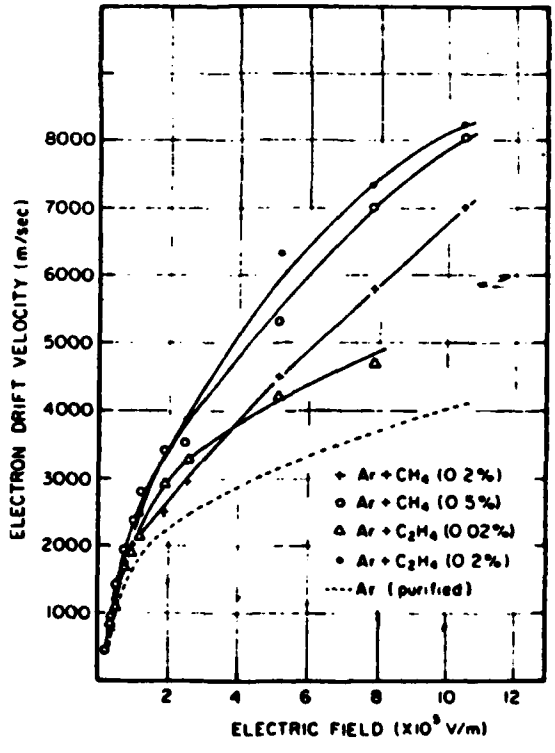

Figure 3. Electron Drift Velocities in Argon Mixtures (Ref 8)

Positive ion drift velocities are less well quantified. Experimental values for some field intensities are shown in table 5. Clearly, the ions drift much more slowly than the electrons. In a 400 kV/m field, for example, the ions would travel at only about 4 cm/sec in liquid argon. This is about five orders of magnitude slower than the electrons. In solid argon, positive ions travel by means of 'hole' conductivity. For the same field strength in solid argon, the ions would travel about two orders of magnitude faster than in the liquid. In both cases the ions are so slow that their movement makes no real contribution to the detected pulse. On the contrary, they accumulate in the medium at high count rates, recombining with some electrons and reducing the size of the detected pulse. Charge accumulation, even in liquid argon at low count rates has been reported (Ref 7).

Table 5. Positive Ion Mobilities in Argon

State	Field Strength (MV/m)	Mobility (X10-7 m^2/V-sec)
Liquid	2.4 - 18.7	2.8 (Ref 21)
Liquid	0.01 - 0.4	0.6 - 0.9 (Ref 9)
Solid	<200	100 (Ref 16)

Recombination. Positive ions accumulating in the detector medium may combine with a drifting electron to form a neutral atom, stopping the electron's contribution to the detected pulse. The probability of recombination is a function of the applied field and the concentration of positive ions in the medium. For heavily ionizing particles such as alpha particles, the high local concentration of charges along the particle path makes recombination more probable (Ref 7). This is much less of a problem for photons and electrons. In these cases,

recombination is controlled by the concentration of positive ions not yet swept out of the medium.

The positive ion concentration in the medium can be estimated as follows. The rate of positive ion creation is:

$$Iin = R\frac{E}{w}$$

where I is the number of positive ions formed per second, R is the number of interactions per second and E is the average energy deposited within each interaction. For a cylindrical detector with an anode along its axis and a cathode at its outer surface, the rate of ion collection is:

$$Iout = Qv2\pi rL$$

where Q is the charge density, r is the radius of the detector, L is the length of the detector and v is the drift velocity of the ions. This equation assumes that the charges are evenly distributed throughout the medium and that all of the charges are free to drift. The drift velocity is:

$$v = S\mu$$

where S is the field strength and μ is the ion mobility. Since at equilibrium:

$$Iin = Iout$$

the charge density can be written as:

$$Q = \frac{R\frac{E}{w}}{2\pi rLS\mu}$$

The equation clearly shows that the positive charge density is a direct function of the count rate and the energy deposited by each particle and an inverse function of the field strength.

In solid argon there is another method of charge accumulation. Positive ions may be trapped in the flaws in the crystal, resulting in a substantially greater charge density (Ref 16). A crystal having more flaws, such as one formed by rapid cooling, will accumulate charges more rapidly. The trapped ions are released very slowly, even after the radiation source is removed. However, the ions can be neutralized by a temporary reversal of the biasing applied to the detector to inject electrons from the anode into the medium.

Electron Trapping. The drifting electrons may also combine with electronegative impurities such as oxygen and nitrogen. Electrons will readily attach to these atoms to produce negative ions. As with the positive ions, these ions drift so slowly that they cannot contribute significantly to the detected pulse. The mean trapping distance, λ for the electrons can be estimated from:

$$\lambda = a \frac{S}{p}$$

where S is the field strength, a is the trapping constant and p is the impurity concentration expressed as a ratio of impurities to argon atoms. For oxygen, the trapping constant is 15×10^{-15} m^2/V for fields from 0.2 to 7 MV/m (Ref 11). For nitrogen, the trapping constant is approximately 200 times larger (Ref 11). For a field strength of 400 kV/m and 1 ppm of oxygen impurities, an electron would be trapped after drifting an average of 0.6 cm.

Electron trapping must be minimized because it reduces the output pulse height and makes the pulse height dependent on where in the detector the electrons were formed. The mean trapping distance should be much larger than the maximum drift distance of the electrons. For a cylindrical cryogenic arson detector with a radius of 0.5 cm, the oxygen concentration should be less than 100 ppb to give a trapping distance of about 6 cm or about 10 times the maximum electron drift distance. Obtaining this purity requires that the detector be constructed of materials that do not emit impurities, that the detector surfaces be carefully precleaned and that the argon be purified beyond the 10 ppm purity of research grade argon.

Statistical Fluctuations in Ion Pair Production

The production of electron-ion pairs in the detector medium is a statistical process where the energy deposited is distributed between ionization and competing processes such as excitation and heating. When the competing processes are less effective, the statistical fluctuation in the number of ion pairs produced is reduced. The value associated with this effect is the Fano factor.

The Fano factor essentially relates the observed detector resolution to that predicted strictly from statistics. As shown in equation 1, the detector medium's contribution to resolution is a function of the Fano factor. This value has not yet been determined experimentally for liquid argon. However, it has been calculated from theory, using the value of w, the Fano formula, the Shockley model and an energy balance equation for the energy deposited in the medium. The calculations gave a Fano factor of 0.107 for liquid argon (Ref 3).

It is the low value of the Fano factor that gives liquid argon its potential for excellent resolution.

Position Effects on Pulse Height

In a cryogenic argon detector, only the electrons drift fast enough to contribute to the pulse height. The charge of the electron and the distance it drifts across the electric field determines its contribution. For an ionization near the anode, the electron drifts only a short distance before being collected. For ionization near the cathode, the electron drifts across the entire field. Thus, the position in the detector at which the particle interacts affects the resulting pulse height. This variation in pulse height with position degrades the energy resolution of the detector.

Experimental Argon Detectors

Over the past ten years cryogenic argon detectors have been studied in detail and applied to several problems in radiation detection and analysis.

One study used a detector consisting of two plates spaced 1.1 cm apart, with a Frisch grid 0.5 cm from the cathode (Ref 5). Using as a source Bi-207 coated on the cathode, the detector gave a resolution of 34 keV FWHM for the 976 keV conversion electron. This is the best resolution reported thus far for a cryogenic argon detector. However, 15 keV was the expected resolution considering electronic noise and the Fano factor. The study demonstrated that conversion electrons can be efficiently detected in liquid argon with fairly good resolution and that argon purity of better than 100 ppb of oxygen and low-noise electronics are essential to achieving this resolution.

Another study used a detector composed of an anode wire 10 microns in diameter stretched through a 0.6 cm diameter cylindrical cathode (Ref 16). The study used both liquid and solid argon as detector media. Using liquid argon, the detector barely had sufficient electronic gain to record the 1330 keV gamma from a Co-60 source. Electron multiplication was achieved with a multiplication factor of about 100; however, the detector operation was extremely unstable at the field strengths required for multiplication. Several interesting observations were made using solid argon as the detector medium. The positive charges move through 'hole' conductivity and travel significantly faster than in the liquid. The flaws in the argon crystal inhibit positive charge collection by trapping the ions. This was the only reference found which discussed in detail solid argon as a detector medium. It suggested that this medium may offer several advantages including more rapid charge clearing, vibration damping and electron multiplication.

One application of liquid argon detectors was a multiple wire detector to give positional information about the event detected (Ref 2). One such detector used an anode composed of strips etched from gold on a sapphire substrate with 20 micron spacing. The cathodes were silver strips painted onto glass and set parallel to, and 2.3 mm from, the anode substrate. Each anode was attached to a separate cooled FET preamplifier. The detector gave 20 um RMS spatial resolution.

The liquid argon detector has also been applied as a total-absorption detector, or calorimeter (Ref 22). The 200 parallel anode and cathode plates were interspaced with 2 mm gaps and immersed in liquid argon to give a total detector length of 70 cm. This was sufficient to detect particles with energies of several GeV. The

advantages of liquid argon as a detector medium in this application is that it is relatively inexpensive, easy to purify, dense and inert.

III. DESIGN AND CONSTRUCTION OF THE DETECTOR

Design Requirements for the First Detector and Gas Handling System

The theory of ionization chamber detectors using cryogenic argon as the detector medium and a study of the argon detectors constructed by other experimenters suggest several requirements for the design of a detector for quantative analysis of xenon. The most important of these requirements are low electronic noise, high purity of the argon medium and good detection efficiency.

The electronic noise of the system must be made as small as possible. The number of ionizations resulting from a 160 keV event, such as from Xe 131m, is extremely small, less than 7000. Compounding this problem are the facts that the positive ions do not contribute to the detected pulse and that impurities can trap the electrons. To counter this, a very sensitive low-noise preamplifier must be used. Also, the capacitance of the cell must be made as small as possible to maximize the signal seen by the preamplifier.

Because of the effect of electron trapping on resolution and detection efficiency, oxygen, nitrogen, fluorocarbons and other electronegative impurities in the detector medium must be kept to a minimum. The oxygen concentration in the argon should be below about 100 ppb to give the electrons a mean free path of about 6 times the cell diameter. Other impurities are less important but should be limited to a few ppm. To accomplish this, the detector must be constructed of materials that can be made as clean as possible and will not outgas impurities.

Further, since the supply of argon and the xenon sample are not pure enough initially, some type of purifier is needed to remove impurities from the gas before it is used in the detector.

Since the xenon source is dispersed in the argon, good detection efficiency requires that all of the argon be used as detector medium. Most of the detectors used by other experimenters have the anode and cathode immersed in a larger volume of argon with only the space between them used as the detection volume. To approach 100 percent detection efficiency, the anode and cathode must surround the argon so that all of it is in the detection volume. Further, since the vapor pressure of liquid argon is high, the gas volume above the detector must be small so that most of the argon will condense.

The following requirements were applied to the design and construction of the first detector and the gas handling system (GHS):

1. Electronic noise must be minimized.
   a. A low-noise, cooled, field effect transistor (FET) preamplifier must be used.
   b. To match the input capacitance of the FET, the capacitance of the detector must be as small as possible.
   c. The distance between the detector and the FET must be minimized.
   d. A very low-noise high voltage power supply, with additional filtering, must be used for detector bias voltage.
2. Electronegative impurities in the detection medium must be minimized.
   a. Oxygen impurities must be below 100 ppb while other impurities must be below about 1 ppm.
   b. The detector must not contain materials which could outgas electronegative impurities (plastics, adhesives, vacuum grease, Teflon).

c. Metal-to-glass seals, which may crack or leak must not be used in the cooled portion of the detector.

d. The detector must be thoroughly cleaned to remove surface impurities and moisture. A vacuum system attached to the detector will help clean the system.

e. A purifier must be installed to purify the gas and maintain its purity. Several passes through the purifier will be necessary.

3. Detection efficiency, particularly for electron emissions, must approach 100 percent.

   a. The entire volume of argon must be between the anode and cathode of the detector.

   b. The amount of argon introduced into the detector must be measurable.

   c. The detector must be large enough to minimize edge losses.

   d. The gas volume above the detector must be minimized.

4. The detector must be cooled to below -190 C. Liquid nitrogen will be used as the refrigerant.

5. The samples will be introduced from breakseal bottles. The breakseal bottles will be filled from a separate system.

Some of the requirements were found to conflict. To keep the FET close to the detector and avoid metal-to-glass feedthroughs, the FET and some associated electronics were placed inside the cell. This meant that the plastic potting material for the FET and some teflon wire insulation had to be put inside the detector. The volume needed for the electronics and the volume of the purifier left a total volume of 563 cc above the liquid argon. Consequently, some of the xenon sample would be dispersed in the argon gas and not immediately seen by the detector.

The xenon would slowly interdiffuse through the argon toward the detector, causing an increase in the detected count rate with time.

Construction of the First Detector and GHS

The first detector consists of a detector cell, a purifier and a transfer reservoir. The GHS consists of a measuring volume, a pressure transducer and a gas manifold with valves. Figure 4 is a block diagram of the system. Figure 5 is a drawing of the first detector cell and the GHS. Figure 6 is a more detailed drawing of the first detector. A detailed description of the components and materials of construction is in appendix A.

First Detector. The detector cell is a vertical glass cylinder with a small nipple at the bottom and a metal flange with electronic feedthroughs at the top. The nipple is silvered on the inner surface and the silver continues in a strip up the side of the cell. The silver is the detector cathode. The anode is a wire attached to the end of a glass tube. The tube is supported from the flange. It passes down through the center of the cylinder and holds the anode wire in the center of the nipple. On the tube just above the anode wire are the FET and some associated electronics. Teflon wires run from the feedthroughs to the electronics while the high voltage lead to the cathode runs through a spring contacting the silver strip. The argon entering the detector condenses at the bottom when the nipple is immersed in liquid nitrogen.

The purifier is an arm attached to the side of the detector cell. The arm is a glass tube filled with titanium and zirconium turnings, surrounded by an electric furnace. The turnings, when heated, collect

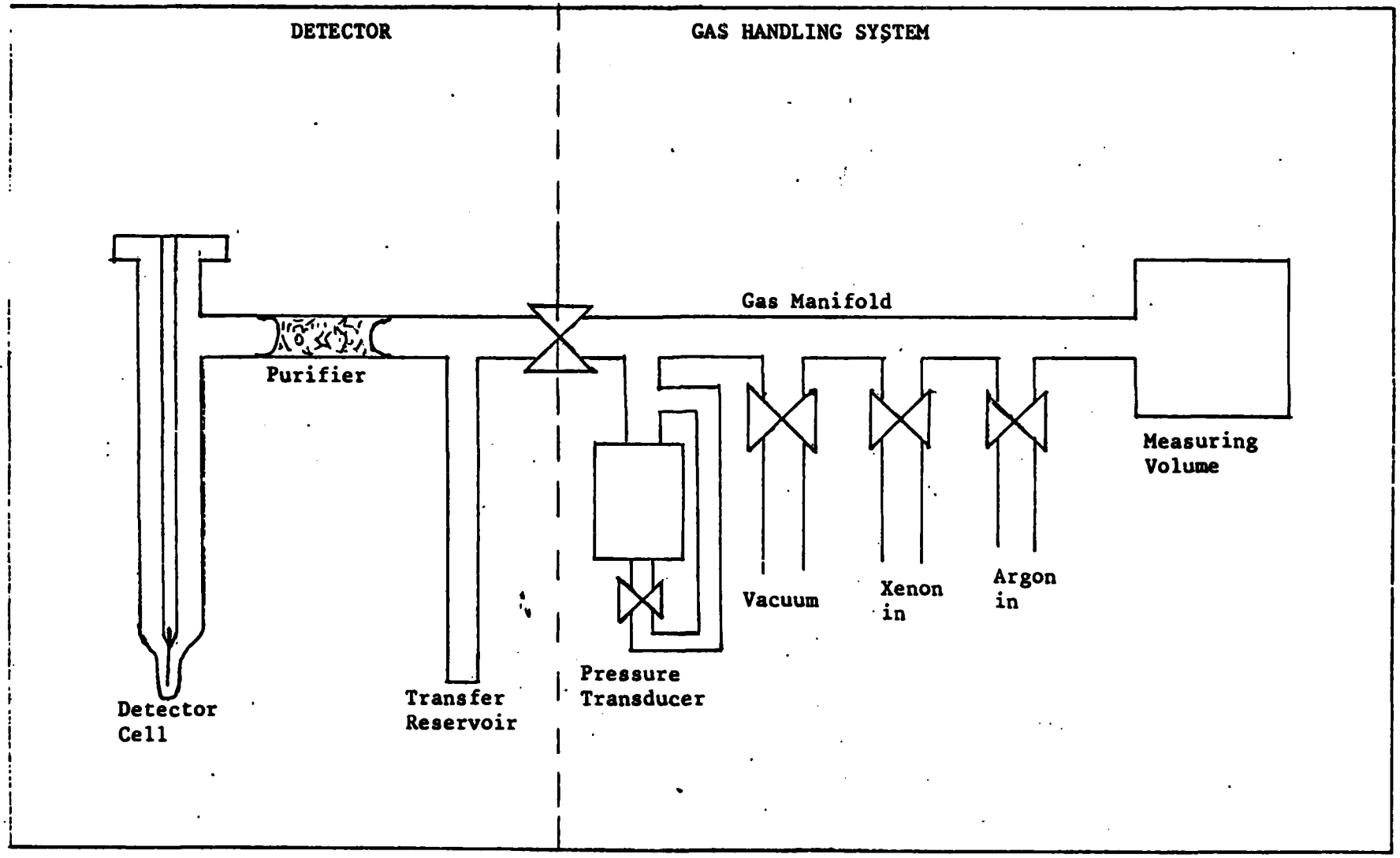

Figure 4. Block Diagram of Detector System

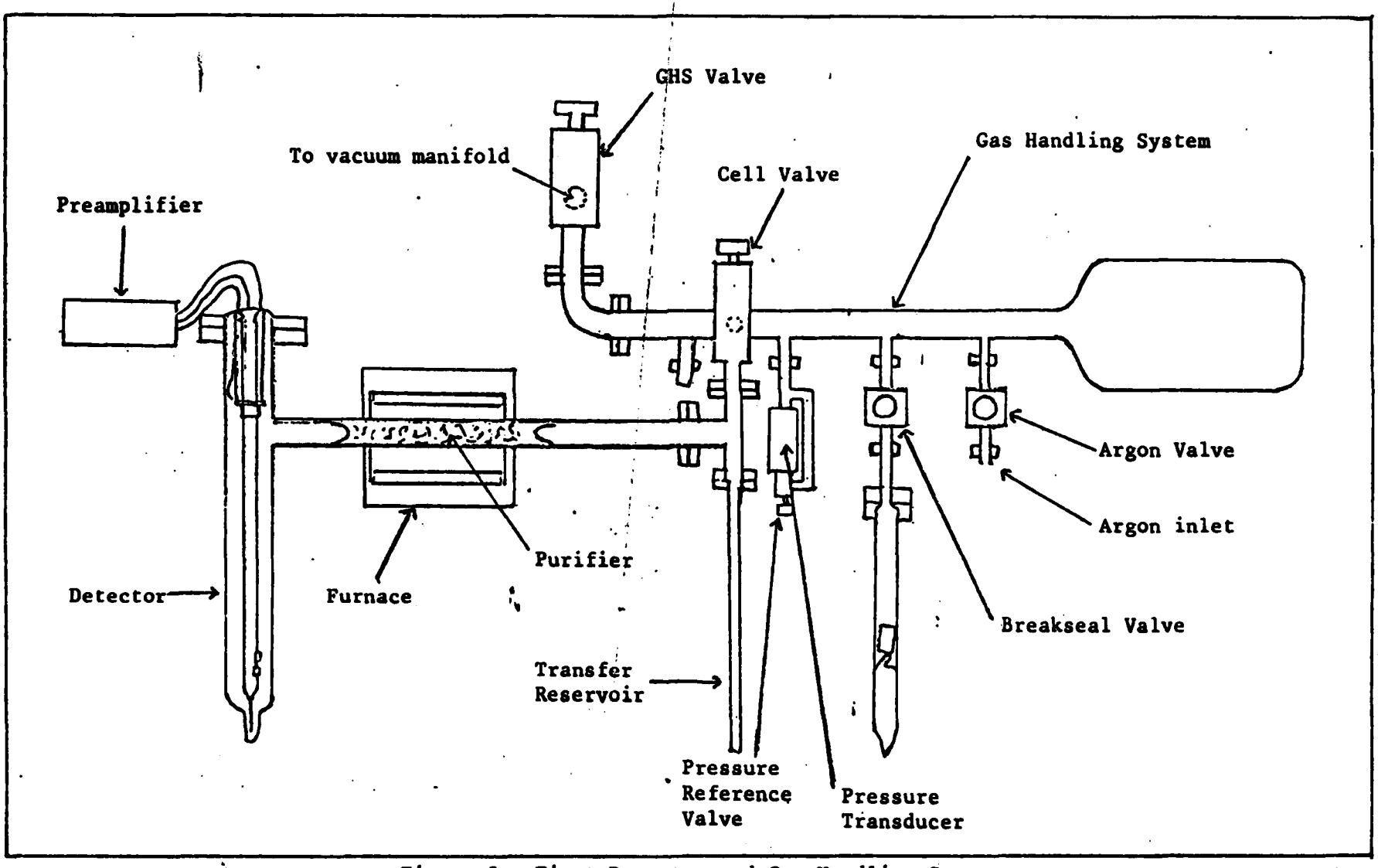

Figure 5. First Detector and Gas Handling System

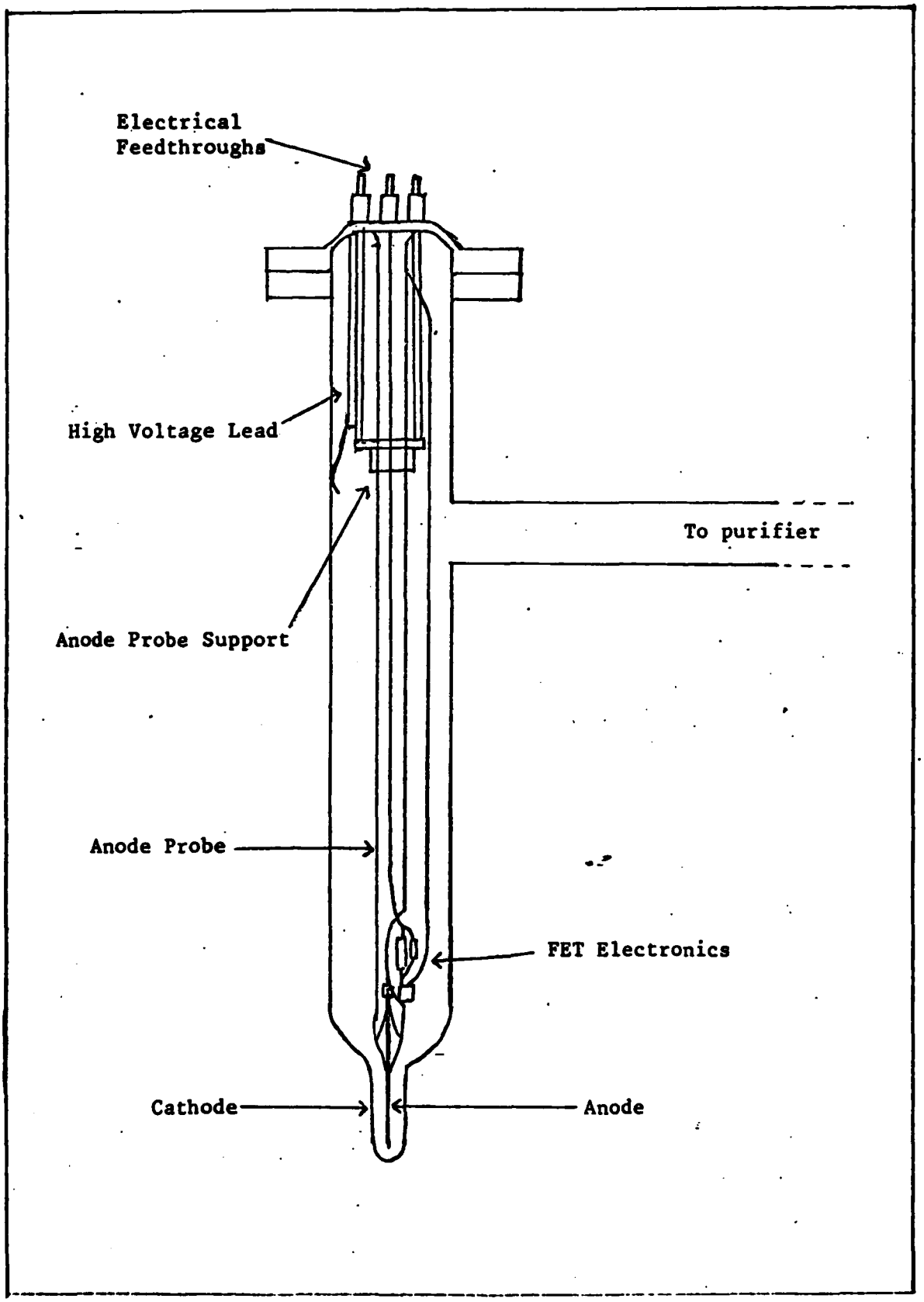

Figure 6. First Detector

oxygen and nitrogen on their surfaces (Ref 6). The argon gas and xenon sample must pass through the purifier to condense in the detector cell.

The transfer reservoir is a vertical tube attached to the side of the purifier opposite the detector cell. It is used primarily to purify the detector medium. When the cell and the reservoir are alternately immersed in liquid nitrogen, the argon and xenon are repeatedly passed through the purifier. Above the reservoir is a valve leading to the GHS.

Gas Handling System. The GHS measuring volume is simply a bottle to provide a calibrated volume of 1.057 liters, including the manifold and valves. The gas manifold is attached to the bottle. Attached to the gas manifold are a vacuum manifold, a breakseal connector used to introduce the sample, a line attached to a supply of 99.999+ percent pure argon, and a connection to the detector. Each of these attachments are through bellows valves. A 0-25 psi relative pressure transducer is also attached. The measured volume and pressure transducer are used to determine the amount of argon being transferred to the detector.

Design Problems with the First Detector

There were several problems with the operation of the first detector. The detector would not accept biasing voltages greater than about 1200 V. The probe vibrated, introducing noise. There was inadequate temperature control and shielding for the detector. Many of the problems could only be eliminated by redesign.

Bias Voltage. The detector was designed to operate at a nominal 1000 V biasing. The resulting field strengths of 100 to 900 kV/m proved inadequate for good charge clearing. When biasing exceeds about 1200 V, breakdown occurs at some point in the system. If the pressure

in the cell is less than about 300 torr, breakdown occurs at about 900 V. A much higher biasing voltage is needed to allow higher count rates and give more complete charge collection.

Vibration. Mechanical vibration of the probe creates low frequency noise of large amplitude. Any lateral movement of the anode changes the capacitance of the detector. This is detected in the preamplifier as a voltage change. The period of the oscillation is about 20 msec but there also seems to be a shorter period oscillation at about 70 usec. The faster oscillations can not be filtered effectively without distorting the signal. Freezing the argon eliminates them completely. However, to operate with liquid argon, a much shorter and stiffer anode is needed.

Temperature Control. To maintain the argon as a liquid, the cell nipple has to be kept just above the liquid nitrogen. As the nitrogen evaporates, the dewar has to be raised to maintain the proper argon temperature. This has to be done every few minutes. Because of the low count rates, a detailed spectrum requires ten hours or more. A more effective means of controlling the argon temperature is required.

Radio Frequency Interference. The detector is extremely sensitive to radio frequency (RF) interference. The detector is surrounded with make-shift RF shielding made of aluminum foil, but this shielding is not very effective against high frequency interference. Permanent, hermetic RF shielding is needed for the cell.

Design Requirements for the Second Detector

The design problems of the first detector were eliminated in the second. The following additional criteria were applied to the design of the second detector cell:

1. The anode vibration must be minimized.
2. The system must be capable of 5000 V biasing.
3. There must be adequate long-term temperature control of the detector.
4. RF shielding must be incorporated.

The requirement for the first detector to avoid metal-to-glass seals was not used for the design of the second detector. Kovar metal-to-glass seals can withstand liquid nitrogen temperatures without leaking or cracking. Eliminating this requirement allowed the detector cell to be made much smaller and allowed the FET electronics to be kept outside the cell.

Construction of the Second Detector

The second detector uses the same GHS and transfer reservoir as the first detector. A new purifier was constructed for the second detector but was identical in design to the first purifier. Figure 7 is a drawing of the second detector. Appendix A contains a detailed description of the components and materials used.

The second detector is a glass and metal cylinder, much smaller than the first detector cylinder, with the electronics mounted above it. The cathode is a kovar metal cup at the bottom. At the top is a Kovar metal ring attached to an electrical feedthrough. The anode is a metal rod extending from the feedthrough and centered in the cup. The entire cell is enclosed in a vacuum chamber whose walls also serve as an RF shield. A copper and boron nitride heat pipe enters through the bottom

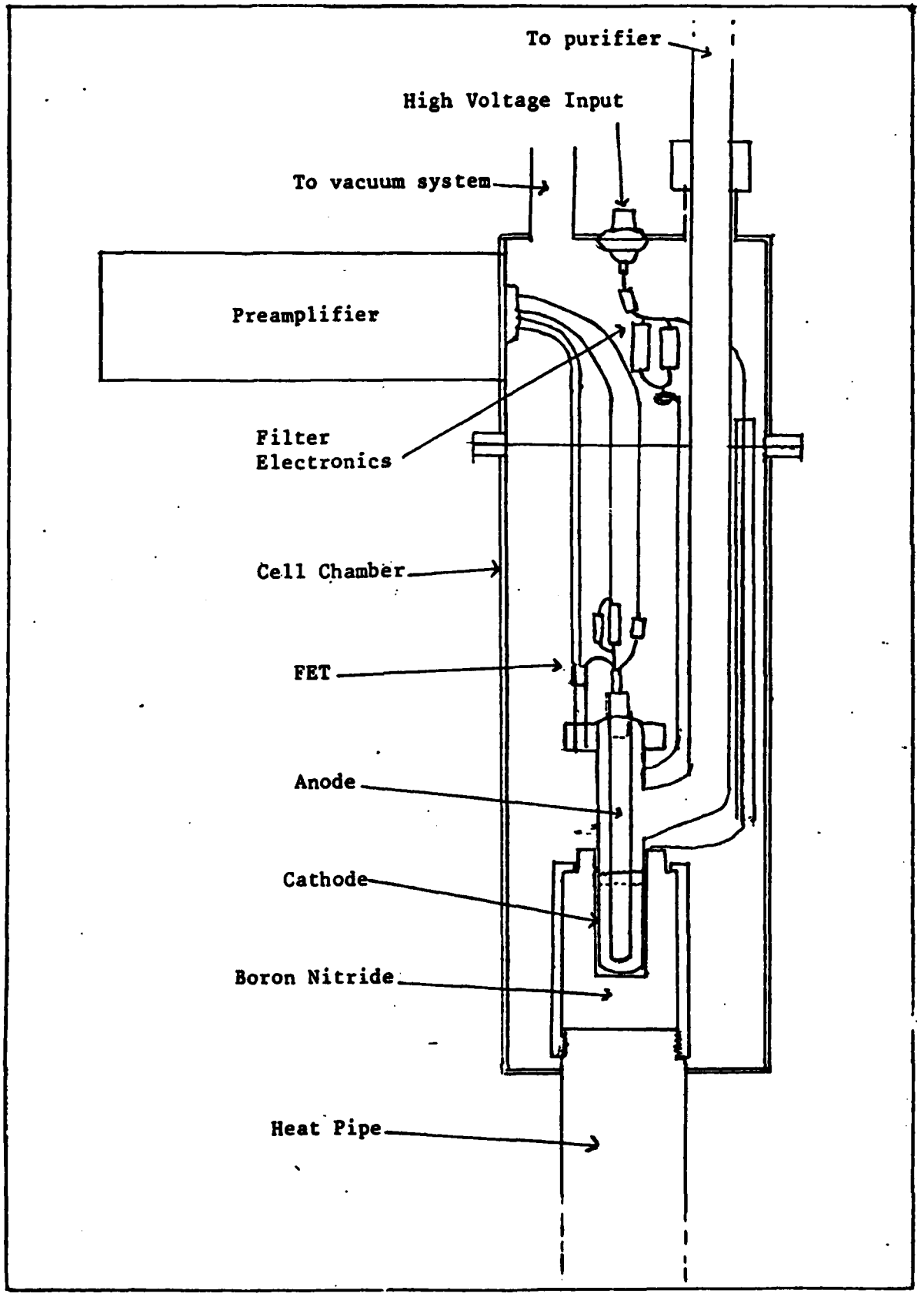

Figure 7. Second Detector

of the chamber to cool the detector cup. The other end of the heat pipe and the lower portion of the chamber is immersed in liquid nitrogen. A thermocouple and heater wire at the top of the heat pipe provide temperature control.

This detector is a significant improvement over the first. It can operate with a liquid argon medium. It can readily be held at temperatures as low as -190 C. Vibrational noise was suppressed by making the anode of 1/8 inch diameter stainless steel rod and by making it much shorter. The larger diameter reduces the variation in the detector field, making the detector more closely approximate a parallel plate detector. It also reduces the possibility of electron multiplication at the small irregularities in the anode. RF interference is greatly reduced; however, some noise can enter through the heater wire and thermocouple wire unless at least one leg of each is grounded. An additional advantage of the new detector is that the FET electronics are more readily accessible.

Electronics

The electronics used with both detectors are shown in Figure 8. It consists of the standard modules used for pulse-height spectrometry: a preamplifier (with cooled FET), a linear amplifier, a multichannel analyzer and a high-voltage power supply for biasing the detector. An oscilloscope was used to monitor the output of the preamplifier and the amplifier.

The preamplifier used in both detectors was salvaged from a commercially manufactured Ge(Li) detector. Its specified sensitivity and noise characteristics made it well suited to this application. However, two transistors and a choke coil had to be replaced before the

preamplifier would operate in the first detector. Afterward, FET drain current and voltage could not be adjusted to specifications and transistors failed repeatedly during operation. When it did operate, its sensitivity and noise characteristics were adequate.

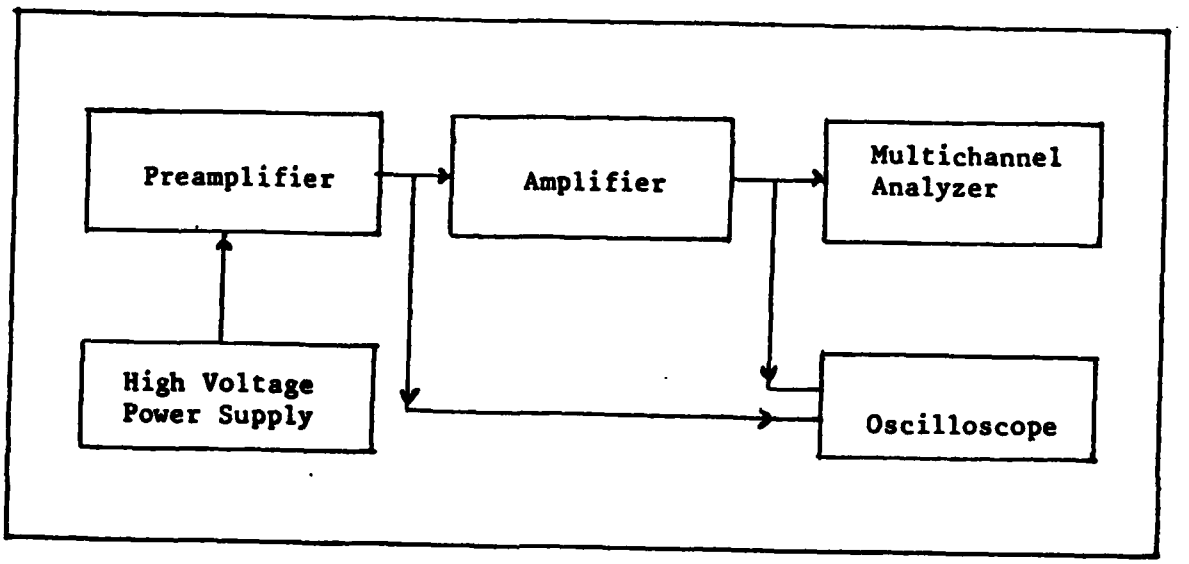

Figure 8. System Electronics

IV. OPERATION, OPERATING CHARACTERISTICS AND RESULTS

Operation

The operation of the two detectors is essentially the same. Only the means of purifying the gas and controlling the temperature of the cell are different. After the system is purged and evacuated, the xenon sample is cryogenically pumped from the breakseal bottle into the transfer reservoir of the detector. Then the measured volume of the GHS is filled with arson and its pressure recorded. The pressure, volume and temperature (assumed 25 C) is used to determine what the liquid volume of the argon would be. The perfect gas law is assumed. That argon is then cryogenically pumped into the transfer reservoir. The procedure is repeated as often as needed to transfer the desired amount of argon (2 to 3 cc) to the transfer reservoir. The mixture is then purified by alternately cooling the detector cell and the transfer reservoir in liquid nitrogen to pump the gas repeatedly through the purifier. Finally, the mixture is liquified or solidified in the cell for analysis. The steps in the operation of the system are listed in appendix B.

Operating Characteristics of the First Detector

Early operation of the first detector was characterized by a very weak response to external gamma sources and no resolution of their energy peak. Later, both improved although the detector never produced a clearly resolved peak. The improvement may be due to a slow surface cleaning process occurring as the argon gas was repeatedly condensed and

evaporated within the detector. The early spectra were very similar to those taken later using poorly purified argon (figure 10a). A collimated external gamma source demonstrated that the detection process was occurring in the liquid or solid argon rather than in the gas above it.

Once the detector began producing a stronger output with some peak resolution, other operating characteristics were investigated. These characteristics included: sources of noise, the noise contribution to resolution and variation in the detector's performance with temperature and pressure. Many of the characteristics limit the performance of the detector.

Sources of Noise. With liquid argon in the cell, low frequency noise of several mV amplitude was seen at the output of the preamplifier. This noise easily swamped any other signal from the detector. As the detector cell was cooled, the noise slowly reduced in amplitude as the freezing point of argon was approached. At the freezing point, the noise increased suddenly and then quieted to less than one mV once the argon was frozen. This noise was caused by mechanical vibration in the probe. The probe responded to vibration of the support stand or table and to the boiling of the nitrogen refrigerant. The sudden increase in noise at argon's freezing point was probably caused by the boiling of the nitrogen as it carried away the argon's heat of crystalization. Because of the vibrational noise, the first detector used solid argon exclusively as its detector medium.

A significant characteristic of the detector using solid argon as the detector medium was the difficulty in reproducing detector performance, particularly efficiencies and detector resolution. This is

attributed to the difficulty in forming crystals of uniform structure. Crystals with few flaws required about 10 hours to form and could not be kept overnight. Crystals formed over about an hour were used for data collection. The performance of these crystals would vary from one crystal to another. Performance also varied with time for the same crystal as it accumulated trapped positive ions.

Reversing the biasing the detector for a few seconds to clear the trapped positive ions temporarily improved its performance. The improvement was accompanied by noise consisting of sporadic pulses much too large to be radiation interaction. This phenomenon has been reported by other investigators and attributed to "capture and release of injected electrons in shallow energy levels in the crystal" (Ref 16). However, they reported that the pulses disappeared after 2-3 minutes. The observed pulses never disappeared but tapered off after a few minutes. Once the large pulses tapered off, they would disappear when the radiation source was removed but return with the return of the source.

Effect of Noise on Resolution. The noise contribution to the FWHM of energy peaks in spectra taken from the first detector could only be estimated. Because of the limited number of electrical feedthroughs, no test pulse input was provided for the detector. However, a pulsar signal fed through a wire leading near the cell would inject a pulse by induction. The contribution of electronic and mechanical noise to peak FWHM was determined from a pulsar spectrum taken in this manner. The spectrum obtained is shown in figures 9a and b. The energy per channel was estimated by assuming that the highest energy pulse seen from the Xe 131m source is 160 keV. The FWHM for the noise is estimated at

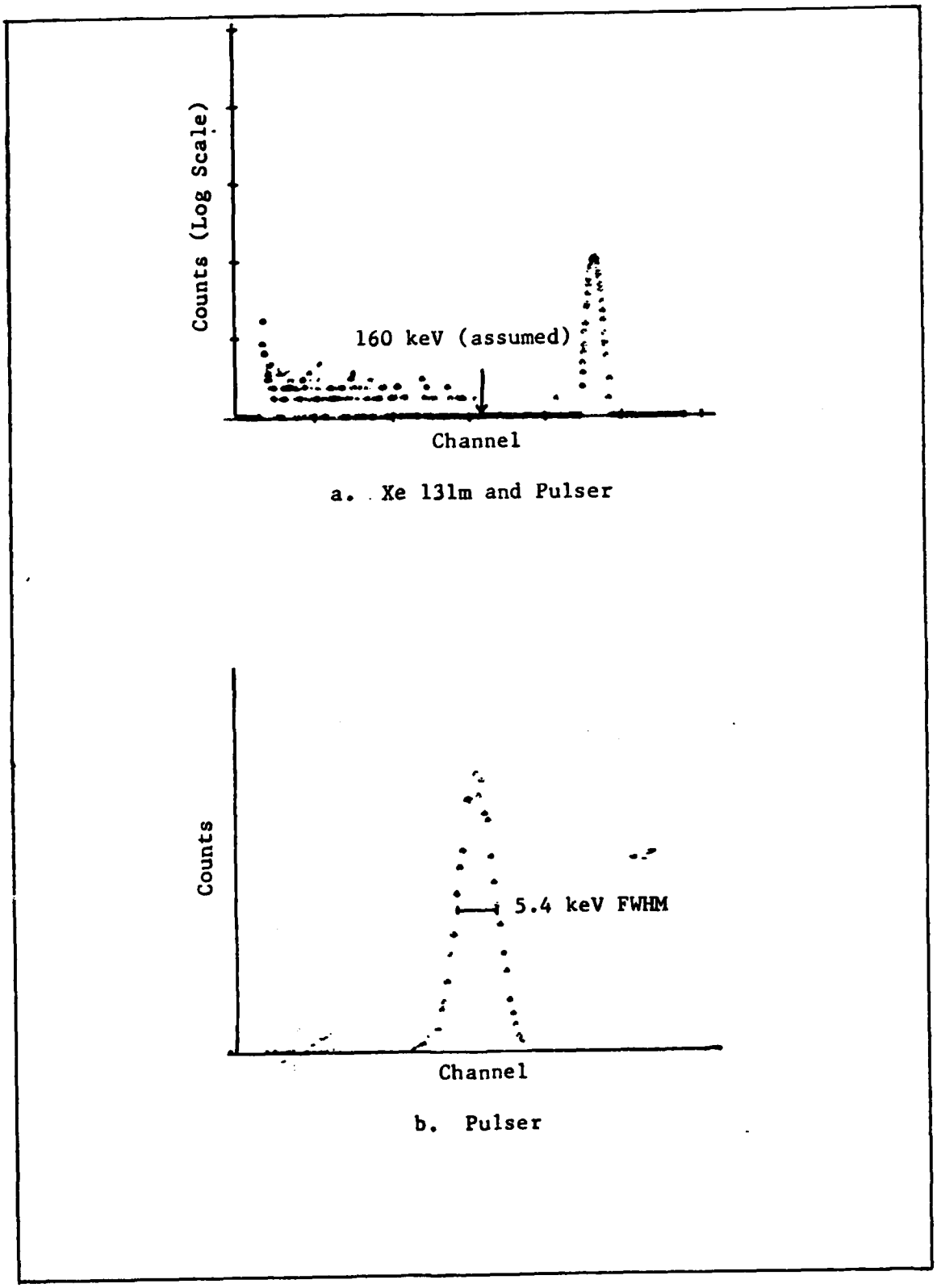

Figure 9. Spectrum of Xe 131m and Pulser

5.4 keV. An estimated +/-30 keV error in the energy calibration gives a noise estimate error of +/-1 keV.

The energy per channel in the spectrum could only be estimated because the detector and electronics could not be accurately calibrated. No clearly recognizable energy peaks could be found in any of the spectra. The gain of the preamplifier was not accurately known because two of its transistors had been replaced. Because the pulsar signal was injected from an unconnected external wire, the capacitance coupling to the anode was unknown. Thus, no feature of any spectra could be related to a specific radiation energy or to the size of an injected pulse.

Temperature and Pressure Effects on Detector Performance. The temperature and pressure of the argon in the detector are related by the vapor pressure of the argon at the cell temperature. The partial pressure of the xenon is negligible near liquid nitrogen temperatures. No temperature sensor was used in the first detector cell. Since temperature control was needed to grow crystals or to keep the argon in the liquid state, the cell valve was left open and temperature was determined from the vapor pressure of the argon as seen at the GHS pressure transducer. Impurities introduced from the GHS were isolated from the cell by the purifier. However, the argon was allowed to warm overnight with the cell valve open to prevent overpressuring the cell. The impurities that accumulated in the argon had to be removed by the purifier before each day's operation. Thus, the concentration of impurities in the argon would vary from day-to-day, affecting both resolution and efficiency.

The vapor pressure of argon in the detector cell also influenced the maximum biasing voltage that could be applied. The point at which high voltage breakdown occurred in the cell was directly related to the

pressure. Since biasing voltage determines the cell's field strengths which determines the rate of positive ion collection and the mean trapping distance of the electrons, the pressure indirectly affected the drift distance of the electrons. Thus, the pressure in the cell could limit the detector's pulse height response to radiation interaction by limiting the biasing voltage.

The argon pressure also limited the detector's efficiency by restricting the movement of the xenon sample to the cell. The xenon, when mixed with the argon gas, does not migrate very rapidly to the cell even though the temperature differential creates a gradient in its partial pressure. The argon impedes the diffusion significantly. At 200 torr argon pressure, the diffusion coefficient for the xenon is calculated to be 0.32 cm^2/sec. At this pressure the xenon would diffuse an average of 1 meter in 6.8 hours. (The diffusion calculations are contained in appendix C.) If the cell were held at a constant temperature, the xenon concentration in the cell would rise very slowly. Cooling the cell would increase the xenon concentration more rapidly as more of the argon-xenon mixture would condense. If the argon medium were solidified, the diffusing xenon would deposit on the surface of the argon or on the cell walls above the argon. Less than 50 percent of that xenon would be detected.

Operating Characteristics of the Second Detector

Most of the negative characteristics of the first detector were corrected in the second. The problem of xenon diffusion through the argon was not corrected. However, the second detector exhibited other negative characteristics related to argon purity and gas handling.

The steps used in cleaning the detector cell after its construction started with rinsing in hot water, deionized water, acetone and finally ethanol. After assembly, the cell was pumped to 10^{-5} torr. This was followed by 5 cycles of pressurization with argon and evacuation. This cleaning process was apparently inadequate. All of the spectra taken from the detector showed what appeared to be the effect of impurities.

The detector used 3 ml of liquid argon. If more argon was placed in the cell, it would not liquify because the top of the detector was not cold enough. The remaining argon pressurized the system, increasing the heat flow into the detector and creating more pressure. Unless the pressure was controlled by cooling the transfer reservoir, the cell could have overpressurized and burst.

During argon purification, the detector was alternately warmed and cooled to move the gas through the purifier. Because of the low coefficient of thermal conductivity between the cell and the heat pipe, the detector cooled very slowly and condensed the argon very slowly. Thus, the transfer reservoir had to be warmed slowly to prevent overpressure. The cell valve was left opened to monitor the cell pressure using the GHS pressure transducer.

Results using the First Detector

The effects of argon purity, temperature and biasing voltage on spectra obtained from an external Am 241 source and internal Xe 131m source were determined. The spectra are shown in figures 10, 11 and 12. In addition, the detector's efficiency in detecting the conversion electrons of Xe 131m was evaluated.

Solid argon was used as the detector medium. Because there is some variation in performance between any two crystals, only the general

pattern of these spectra can be compared. This is particularly true of purity analysis results where the argon was evaporated, purified and recrystalized between each spectrum collection.

Effects of Purity. The effect of increasing purity on the spectrum of Xe 131m can be seen in figures 10a, b, c and d. Horizontal and vertical scale and counting times are identical for the spectra. The most significant effect is the improvement in resolution with increasing purity. The count rate also increased by 30 percent from spectrum a to d, with most of the increase from a to b. The impurities appear to spread the peak pulses over the lower channels, with some of the pulses lost below the lower level discriminator of the multichannel analyzer.

Effects of Temperature and Time. The effects of time and temperature on the spectrum of Xe 131m can be seen in figures 11a, b, c and d. Horizontal and vertical scale and counting times are identical for the spectra. The spectra show that low pulse height counts are increasing steadily with time and reduced temperature. This is most likely the effect of increasing positive charge saturation with time. The increase in the count rate is probably a function of temperature. As the temperature is reduced, more argon and xenon is condensed into the detector giving a higher count rate and relatively more counts in all channels.

Effects of Biasing Voltage. The effects of different biasing voltages on the spectrum from an external Am 241 source can be seen in figures 12a, b, c and d. The higher biasing voltage gives a sharper peak with more high pulse height counts. Since the mean trapping distance is a function of the applied field, impurities have less effect

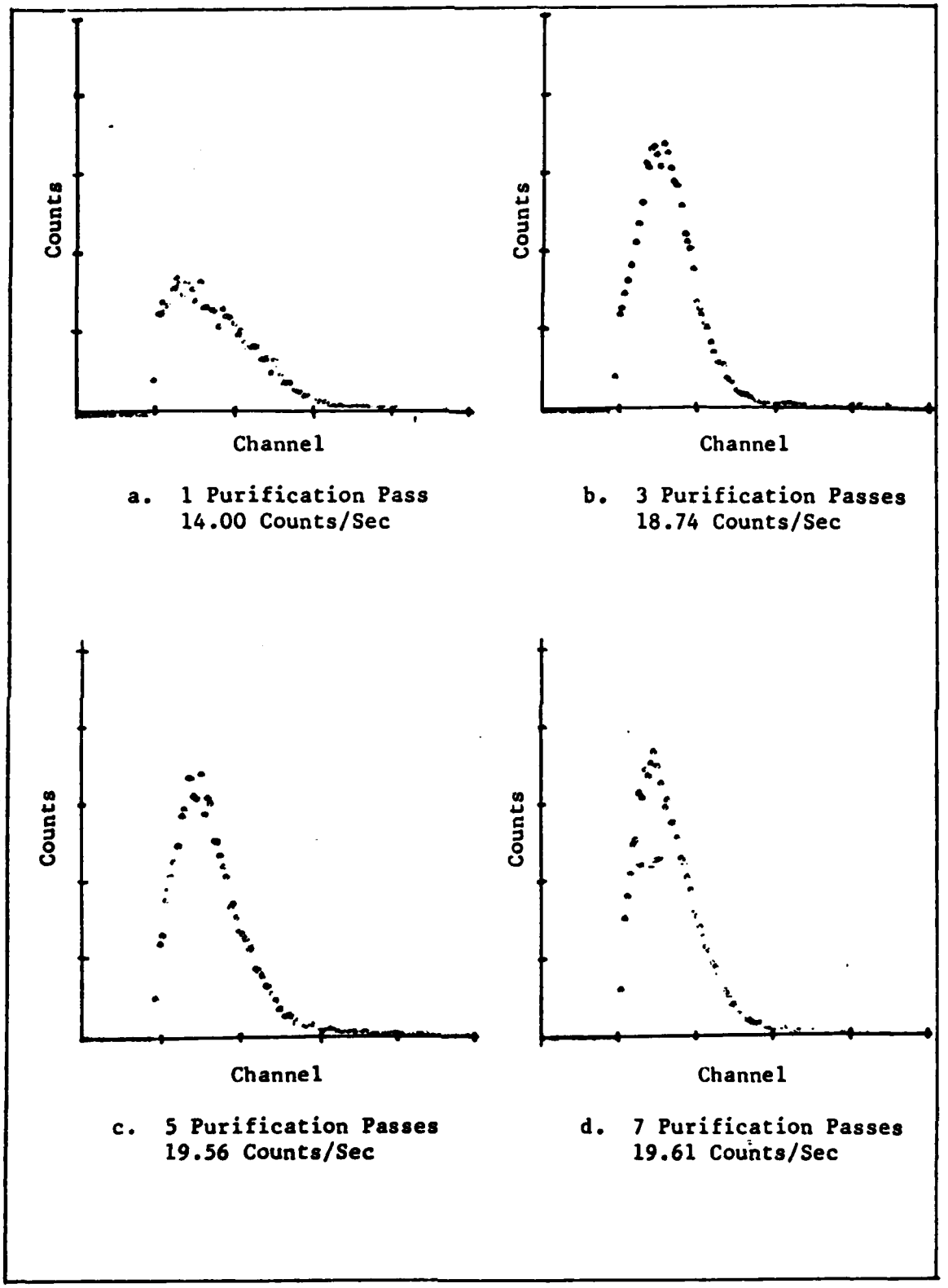

Figure 10. The Effects of Purification on the Spectrum of Xe 131m

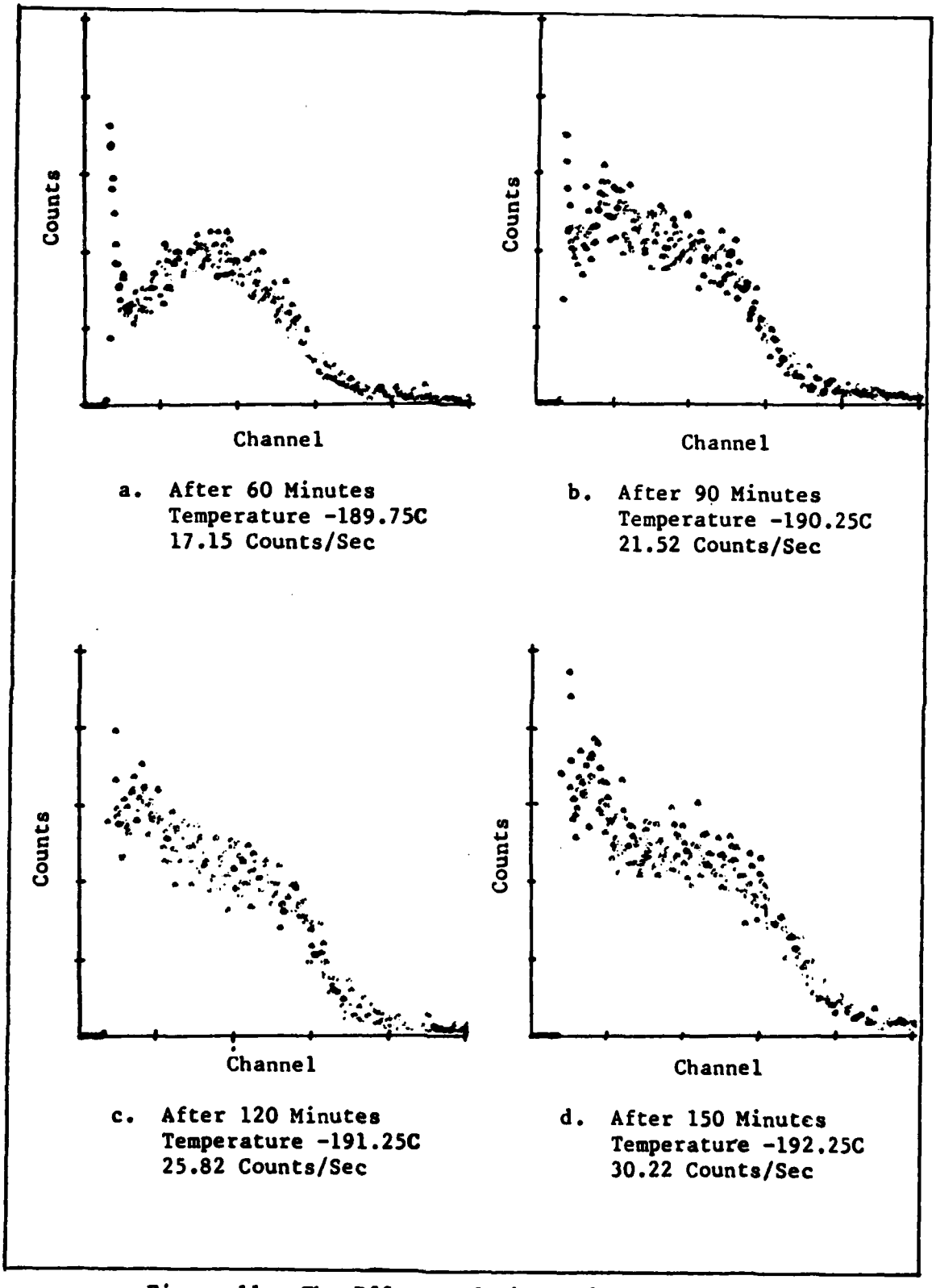

a. After 60 Minutes
Temperature -189.75C
17.15 Counts/Sec

b. After 90 Minutes
Temperature -190.25C
21.52 Counts/Sec

c. After 120 Minutes
Temperature -191.25C
25.82 Counts/Sec

d. After 150 Minutes
Temperature -192.25C
30.22 Counts/Sec

Figure 11. The Effects of Time and Temperature on the Spectrum of Xe 131m

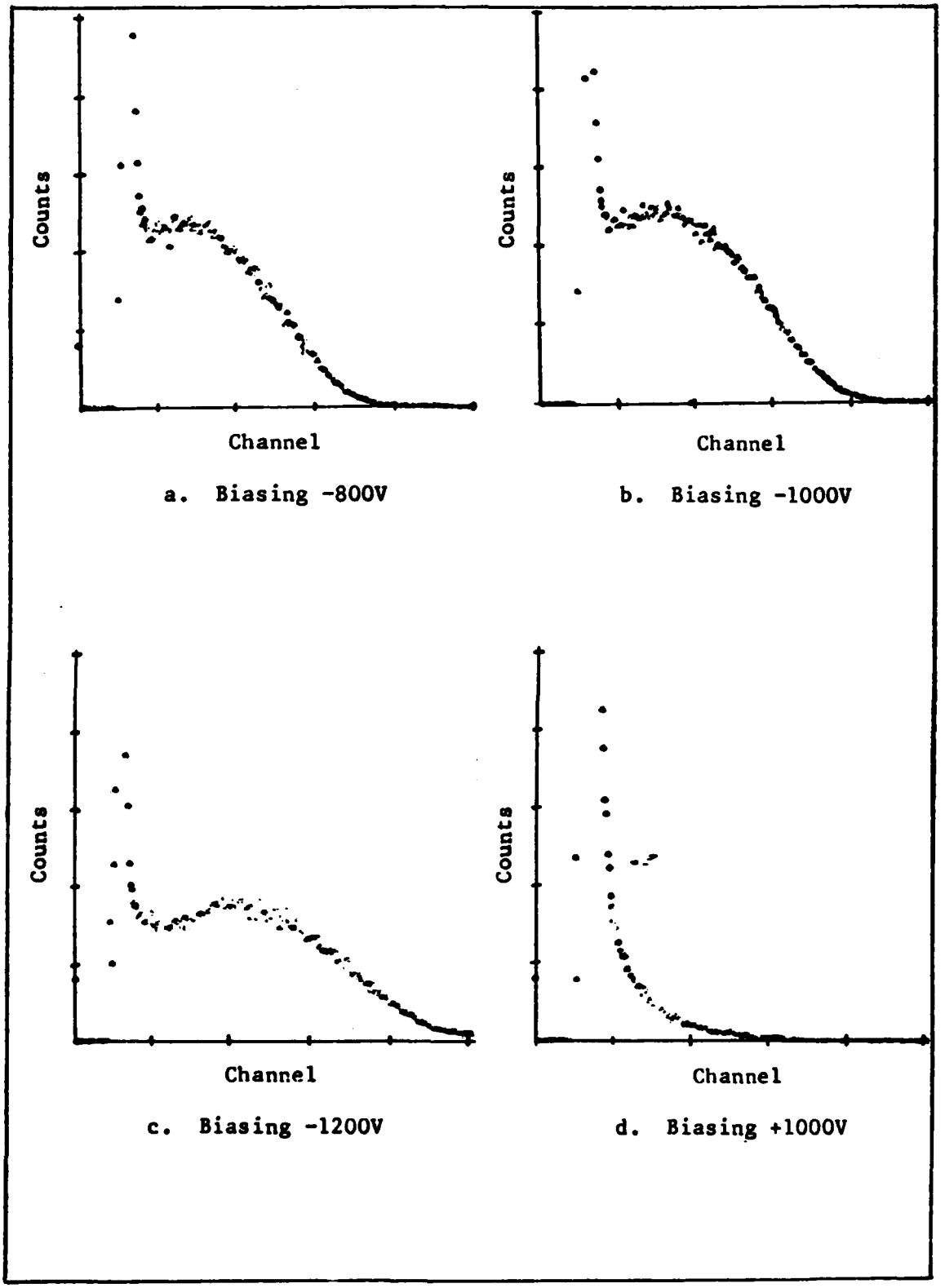

Figure 12. The Effects of Biasing Voltage on the Spectrum of Am 241

at the higher biasing voltages. Further, positive ion collection is improved at higher biasing voltages, reducing recombination.

Positive biasing results in a much different spectrum. Comparison of figure 12b with 12d indicates that positive biasing gives much lower average pulse heights. This could be explained by the geometric effects of a cylindrical detector. For a given radiation energy, the distance the electrons drift to the anode and the strength of the field through which they drift determine the resulting pulse height. With negative biasing, electrons drift toward the central anode. If the radiation interactions are spread uniformly throughout a cylindrical volume, most of the interactions will occur near the surface and their pulse height contribution will be greater because they drift across a larger fraction of the anode-cathode distance. Further, because the field strengths in a cylindrical detector are greater near the center, drifting in that region contributes more to the overall pulse height than does drifting near the outer surface of the detector. Thus, negative biasing results in a larger fraction of the electrons produced contributing more to the pulse heights. The reverse is true for positive biasing since the electrons drift toward the surface of the cylinder. The extreme difference between figures 12b and 12d show the geometric effects of the biasing of a cylindrical detector.

Detector Efficiency. None of the Xe 131m spectra contained the predicted number of counts. The sample was estimated to have an activity of about 300 Bq. Count rates for the spectra were between about 15 and 30 counts per sec. More than 90 percent of the events were lost. Many of the events may have been lost in the noise. It is also possible that most of the xenon was trapped outside the detector medium. Because of

its higher freezing point, the xenon may have been frozen onto the cell walls above the detector or concentrated in the transfer reservoir when the argon boiled away.

Results using the Second Detector

The second detector, using liquid argon as the medium, gave no noticeable response to an internal Xe 131m source. It did show response to an external Co 60 source but gave only pulses of apparently random height to a maximum of about 1 mV from the preamplifier. Since these pulses should correspond to a maximum energy of 1330 keV, pulses corresponding to the 160 keV electron of Xe 131m would be lost in the noise. The spectra obtained from this detector are very similar to those seen for the first detector when it was first operated and many of its impurities had not been removed. The system will probably require baking under vacuum and more extensive purging with argon before it will give significant results.

V. DISCUSSION, CONCLUSIONS AND RECOMMENDATIONS

Discussion of the Results

The response of the detectors is controlled by the concentration of impurities in the detector medium, the concentration of positive ions in the medium, the detector's temperature, and the detector's geometry. Each of these factors affect the resolution and efficiency of the detector.

The most significant aspect of the pulse-height spectra shown in the results is that none of them show peaks that approach the expected resolution. Based on the theoretical detector resolution and the noise estimate, the 164 and 130 keV peaks of Xe 131m would be expected to have about 5.8 and 5.7 keV FWHM respectively. The peaks should be easily distinguishable but are not resolved in figure 10d, which is the spectrum from Xe 131m with the best resolution. Clearly some other factor is seriously degrading resolution. The most likely factors are impurities, positive ion trapping in the solid argon, and the geometry effects of a cylindrical detector.

The efficiency of the detector for the electrons from Xe 131m was far below that expected. Either most of the ionization electrons are not contributing enough to the pulse-height for the resultant pulse to be seen above noise, or the xenon is not being efficiently transferred into the detector. Both impurities and trapping would attenuate the pulse-height while the xenon diffusion rate, controlled by detector temperature, would affect xenon transfer.

Effect of Impurities. The effect of the impurities on resolution is clear; they reduce the pulse-height of the detected pulse by a factor that is a function of where in the cell the ion pairs are formed. This tends to spread out an energy peak and move it lower. The purifier effectively removes most of the impurities but they reaccumulate. The Teflon, plastics and small amounts of moisture in the system are the most likely sources of impurities in the first detector. The second detector has no Teflon or plastics and the moisture may be removed by baking. Once the second detector is thoroughly cleaned, its resolution will probably improve significantly. However, the other factors controlling resolution, particularly geometry, will still be present.

Effects of Positive Ion Concentration. Like impurities, the positive ion concentration in the medium will reduce the pulse-height. The ion concentration in the liquid argon is controlled by the detector field strength, a function of detector biasing. It is also controlled by the decay rate of the sample and the energy of its decay. Since the effects of ion concentration in the liquid medium is identical to the effects of impurities, its contribution to the poor performance of the second detector could not be evaluated. In the first detector, using solid argon, positive ion concentration is controlled by positive ion trapping.

Positive ion trapping occurs only in the solid argon medium. The number of potential trapping sites is determined by the regularity of the argon crystal, which in turn is determined by the rate at which the argon is cooled (Ref 16). The effect of the positive ions is very similar to the effect of impurities except that the ions accumulate over time and can be temporarily removed by reverse biasing. The time effects

of positive ion accumulation can be seen in the change in shape of the spectra in figure 11. Reverse biasing can temporarily clear the accumulation but has a disadvantage in that it causes spurious signals.

Temperature Effects. The efficiency of the detector is apparently a function of temperature. The count rates at which the spectra in figure 11 were collected almost doubled with a reduction of 2.5 degrees over 90 minutes. Since the xenon sample was mixed into the argon medium, it seems clear that the xenon in the detector is not uniformly distributed. It is initially in low concentration in the detector cell but increases slowly as the temperature is reduced and time progresses. The slow rate of xenon diffusion through argon would explain the slow increase. The rate of diffusion, controlled by the pressure of the argon, would thus be a function of the detector temperature. This explanation would require that the xenon be initially trapped outside of the detector cell, rather than move and condense with the argon.

There are two possible ways that the xenon could be trapped outside the detector cell. First, as the xenon-argon mixture evaporates from the transfer reservoir, the argon, having a higher vapor pressure, would evaporate first and leave a high xenon concentration in the reservoir. This xenon would then slowly diffuse toward the detector cell because of the partial pressure gradient. Second, as the argon-xenon mixture enters the detector cell, the xenon may freeze onto the walls of the detector above the anode and cathode. From there the xenon would contribute little to the detection efficiency. Because the temperature is slightly higher above the cell, the xenon would slowly move down into the cell. Either or both of these effects may explain the low but slowly rising count rates seen in figure 11.

Geometric Effects. In an ionization detector where only the electrons contribute to the pulse, the pulse height is a function not only of the energy deposited but also where in the detector the energy is deposited. The pulse height is proportional to the number of electrons formed times the average fraction of the total interelectrode potential they drift across. Electrons formed near the anode will drift only a short distance while electrons formed near the cathode will cross almost the entire interelectrode gap. In a parallel plate geometry and for a monoenergetic source, the pulse-height distribution would be constant from zero height to a maximum corresponding to full contribution by the electrons. There would be no peak.

With a cylindrical geometry detector having the anode at its axis, there would be a peak. Assuming that the interactions are uniformly distributed throughout the medium, most of the electrons would be formed near the cathode to give a near-maximum pulse height. Only a small fraction of the electrons would be formed near the anode to give a small pulse. The resulting pulse-height distribution would start at zero, slope upward to a maximum at maximum contribution, and immediately drop again to zero. If the cathode were at the cylinder axis, the distribution would be maximum at zero pulse height and slope downward to zero at maximum contribution. A comparison of these idealized distributions to figures 12b and 12d, respectively, gives some indication of the strong effect of geometry on resolution. Although clearly other effects (impurities, recombination and electronic noise) are degrading resolution, geometry seems to be the most important contributor.

Conclusions

The reasons for investigating the argon detector are that it offers a better combination of resolution and efficiency than the existing methods of analyzing xenon. The conclusions to be drawn concern whether the detectors tested have the resolution and efficiency anticipated.

The first detector, using a solid argon medium, can detect the internal conversion electrons of Xe 131m. However, its resolution is inadequate to resolve the 130 keV K electrons from the 164 keV L,M electrons. The detector can also detect gammas from an external source but cannot resolve a clear energy peak. Its poor resolution is probably the result of geometry factors, impurities and irregularities in the argon crystal medium.

The second detector, using a liquid argon medium, can detect energetic gammas from external sources such as the 1170 and 1330 keV gammas of Co 60. It cannot resolve the two energies. It cannot detect the electrons of Xe 131m, probably because their energy is too low to be seen above the noise. Its poor detection and resolution capabilities are probably the result of a high concentration of impurities in the argon and geometric effects. The cleaning and purging procedures used on the cell were inadequate.

As designed, the detectors will not produce resolution adequate for quantative analysis. The geometric effects will always spread pulse heights toward zero. For good resolution, the detector must be designed such that the pulse-height resulting from an interaction is independent of the position of interaction.

Neither detector accurately measures the quantity of xenon 131m in the sample. The count rates recorded are 10 percent or less of the

sample's activity. This may be because most of the sample is trapped elsewhere in the system and diffuses slowly through the argon.

None of the results indicate whether or not cryogenic argon detectors can be used for quantitative analysis of mixtures of Xe 131m and Xe 133. In theory they will perform better than the scintillation counters currently used. Geometric effects must be eliminated and the xenon sample must be more reliably introduced into the detector.

Recommendations

Cryogenic argon detectors still offer a theoretical advantage in the quantitative analysis of xenon radionuclides. The second detector should be used to investigate further the properties of argon as an ionization chamber medium. A new detector should also be designed to eliminate geometric effects.

Continued Work with the Second Detector. The following recommendations are made to assist work with the second detector:

1. Impurities on Cell Walls. The cell should be baked under vacuum for several hours and then left on the ion pump for several days. It should then be purged with argon and again pumped to high vacuum. The eventual vacuum attained should be better than 10^{-7} torr.

2. Axial Symmetry of the Anode. The anode probe was installed at a slight angle to the centerline of the cell. This creates a nonuniform field in the detector cell. This could limit the cell's maximum biasing voltage or distort the cell's charge collection rates. The probe may possibly be straightened by bending from outside but more likely the cell will have to be resoldered. Another cell, properly aligned but with a smaller anode probe, is available.

3. Reliability and Characteristics of the Preamplifier. Repair or replace the preamplifier. The present preamplifier had to be repaired repeatedly and still cannot be adjusted to its recommended drain current and voltage settings. Evaluation of the second detector was interrupted by an apparent failure of the FET.

4. Use of Xenon as a Detector Medium. Xenon has a lower w and a lower Fano factor, both signal amplitude and resolution should be improved. The use of xenon will eliminate the problems of diffusion and mixing of the sample and medium. Its higher melting point should also make it easier to handle.

5. Improvement of the Detector's Low Temperature Capability. Presently the cell will reach -190C. Since the thermocouple is in the boron nitride, the detector itself is slightly warmer than that. If the cell can be made a few degrees colder, the argon can be solidified. Solid argon offers some advantages as a detector medium. Lower cell chamber pressures and better radiation shielding may be needed to lower the temperature. Turning off the furnace may help. A small amount of boron nitride powder in the detector well may improve conductivity between the boron nitride crystal and the detector. Oil or grease should not be used since they will form a vacuum seal and prevent opening of the cell chamber.

A New Detector Design. The most commonly used method of eliminating position dependence in a detector is with the use of a Frisch grid (Ref 13). The grid is placed between the anode and cathode with the source between the grid and the cathode. The grid is biased so that the electrons will drift toward the grid. When they reach the grid, the grid-anode potential causes them to drift through the grid to the anode.

The signal resulting from the grid-to-anode drift is independent of where the electron was formed. The resulting signal is independent of geometric effects. Because the grid and anode must be carefully aligned, Frisch grids are generally used only on parallel plate detectors.

The detector shown in figure 13 uses a Frisch grid and parallel plate design. It also uses pressurized nitrogen as the coolant. With the nitrogen pressure controlled at about 40 psi, precise temperature control can be maintained without heaters or thermocouples. Using this, or a similar design, the geometric effects can be eliminated and significantly better resolution achieved. By also using xenon as the detector medium, the efficiency, signal amplitude, and resolution may be sufficient to make this type detector suitable for quantative analysis of radioactive xenon.

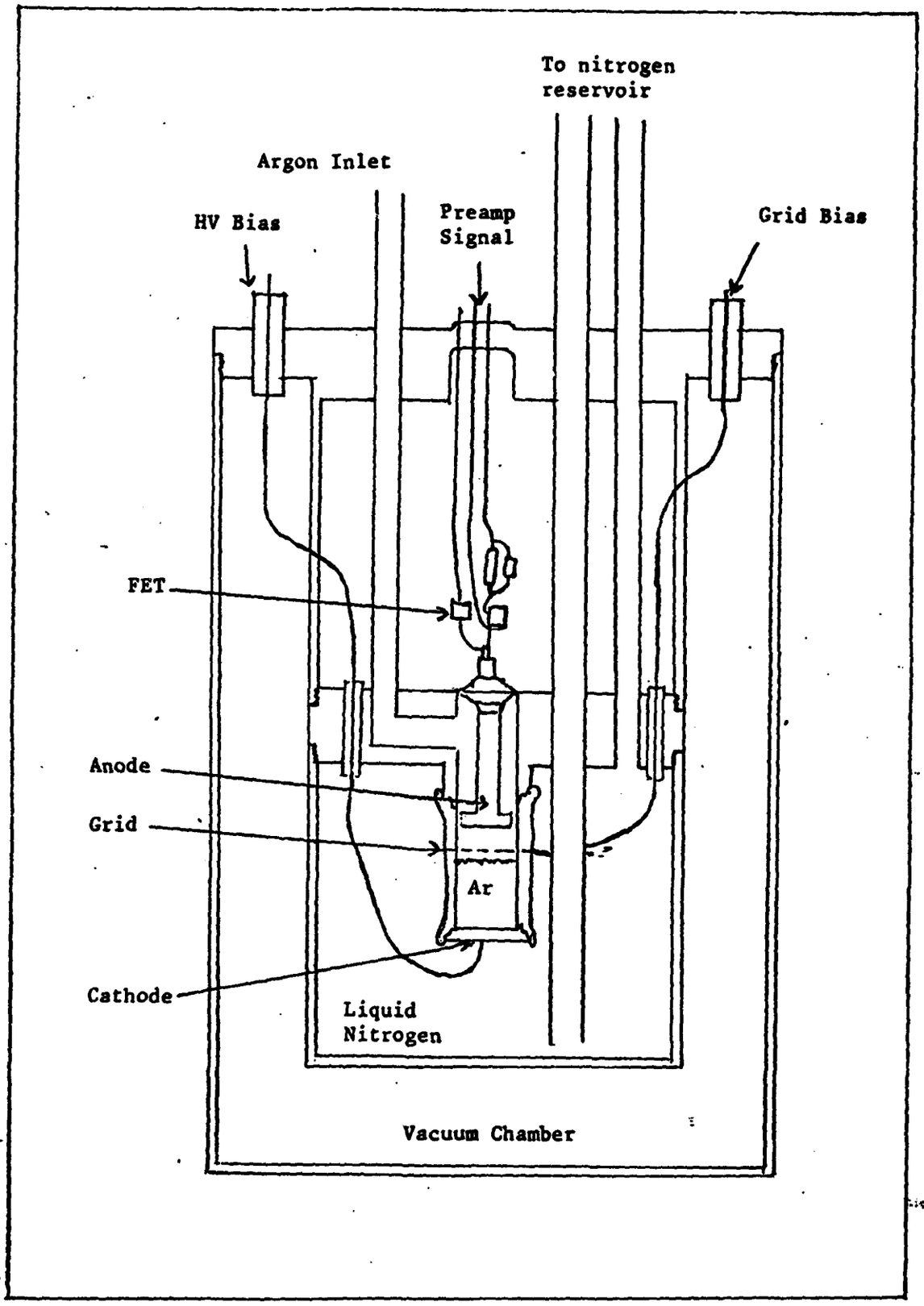

Figure 13. Proposed Detector Design

BIBLIOGRAPHY

1. Brassard, C. "Liquid Ionization Detectors," Nuclear Instruments and Methods, 162: 29-47 (1979).

2. Derenzo, S. E., et al. "Test of a Liquid Argon Chamber with 20 um RMS Resolution," Nuclear Instruments and Methods, 122: 319-327 (1974).

3. Doke, T., et al. "Estimation of Fano Factors in Liquid Argon, Krypton, Xenon and Xenon-doped Liquid Argon," Nuclear Instruments and Methods, 134: 353-357 (1976).

4. Dushman, S. Scientific Foundations of Vacuum Technique (Second Edition). New York: John Wiley and Sons, Inc. 1962.

5. Edmiston, M. D. and C. R. Gruhn. "Energy Resolution Considerations in Liquid Ionization Chambers," IEEE Transactions in Nuclear Sciences, NS-25: 352-353 (February 1978).

6. Gibbs, D. S., et al. "Purification of the Rare Gases," Industrial and Engineering Chemistry, 48:2: 289-296 (February 1956).

7. Gruhn, C. R. and M. D. Edmiston. "Germinate Recombination of Alpha Particle-Excited Carriers in Liquid Argon," Physical Review Letters, 40:6: 110-119 (February 1978).

8. Gruhn, C. R. and R. Loveman. "A Review of the Physical Properties of Liquid Ionization Chamber Media," IEEE Transactions on Nuclear Science, NS-26:1: 110-119 (February 1979).

9. Henson, B. L. "Mobility of Positive Ions in Liquified Argon and Nitrogen," Physical Review, 135:4A: 1002-1008 (August 1964).

10. Hodgman, C. D., editor. Handbook of Chemistry and Physics (44th Edition). Cleveland, Ohio: Chemical Rubber Co. Press, 1973.

11. Hofmann, W., et al. "Production and Transport of Conduction Electrons in a Liquid Argon Ionization Chamber," Nuclear Instruments and Methods, 135: 151-156 (1976).

12. Horrocks, D. L. and M. C. Studier. "Determination of Radioactive Noble Gases With a Liquid Scintillator," Analytical Chemistry, 36:11 (October 1964) 2077-2079.

13. Hunt, K. K. Analysis of a Semiconductor Detection System for Measuring Radioactive Noble Gases. Unpublished Thesis. Wright-Patterson Air Force Base, Ohio: Air Force Institute of Technology, December 1976.

14. Knoll, G. F. Radiation Detection and Measurement. New York: John Wiley and Sons, Inc., 1979.

15. Lederer, C. M., et al. Table of Isotopes (Sixth Edition). New York: John Wiley and Sons, Inc., March 1968.

16. Pisarev, A. F., V. F. Pisarev and G. S. Revenko. "A new Particle Detector - The Crystal Filament Counter," Soviet Physics JETP, 36:5: 828-834 (May 1973).

17. Price, W. J. Nuclear Radiation Detection (Second Edition). New York: McGraw-Hill Book Co., 1964.

18. Rowe, C. R. Quantitative Analysis of Radioactive Noble Gases with a SiLi Detector. Unpublished Thesis. Wright-Patterson Air Force Base, Ohio: Air Force Institute of Technology, March 1974.

19. Shibamura, E., et al. "Drift Velocities of Electrons, Saturation Characteristics of Ionization and W-values for Conversion Electrons in Liquid Argon, Liquid Argon-Gas Mixtures and Liquid Xenon," Nuclear Instruments and Methods, 131: 249-258 (1975).

20. Takahashi, T., et al. "The W-Value of Liquid Argon," Physics Letters, 44A:2: 123-124 (21 May 1973).

21. Williams, R. L. "Ionic Mobilities in Argon and Helium Liquids," Canadian Journal of Physics, 35: 134-146 (1957).

22. Willis, W. J. and V. Radeka. "Liquid Argon Ionization Chambers as Total-Absorption Detectors," Nuclear Instruments and Methods, 120: 221-236 (1974).

APPENDIX A

DESCRIPTION OF THE CRYOGENIC ARGON DETECTOR SYSTEM

The cryogenic argon detector system is a system for cooling purified argon to the liquid or solid state and using the argon as an ionization chamber detector medium to spectrographically analyze radiation sources. The detector system consists of three components: a gas handling system (GHS), a detector cell, and electronics.

Two detectors and a GHS were constructed. Figure 5 is a drawing of the first detector and GHS. Figure 6 is a detailed drawing of the first detector. Figure 7 is a drawing of the second detector. Figure 8 is a diagram of the system electronics.

Gas Handling System

The GHS consists of a manifold having four 1/4 inch tube ports, one 1/2 inch tube port, one 3/4 inch tapered thread pipe fitting and one 3/4 inch copper gasket flange port. Of the four 1/4 inch ports, one is sealed with a swage-lok fitting and cap. The other three are swage-lok fitted to bellows valves. One valve goes to a 25 PSI capacity relative pressure transducer. The reference side of the gage is also connected here but has a separate valve. The second port and valve attaches, through a swage-lok fitting, to a break-seal bottle connector. This connector is for introducing measured amounts of radioactive gas to the system for analysis. The third valve connects through polypropylene tubing to an ultra-high purity argon gas

bottle. The fittings are attached with swage-loks and a pressure regulator controls pressure in the line.

The flange port is connected through a 90 degree elbow to a bellows valve. The valve connects to a vacuum system consisting of a mechanical pump and an ion pump. The pump system is used to purge the system and to provide the reference vacuum for the pressure gage. The pipe fitting is connected to a carbon steel gas bottle having approximately one liter volume. The joint is sealed with teflon tape. The bottle provides system volume for measuring out the argon gas for the cell. The 1/2 inch port leads to the detector cell.

First Detector Cell

The detector cell consists of a transfer reservoir, a purifier and a detector. The valve connecting the GHS to the detector cell is the only inlet to the cell. The O-ring connector on the GHS side of the valve is the only nonmetal seal in the cell. All other connections in the cell are either welds, soldered joints, metal-to-glass seals or copper gasket seals. This is to keep the cell, particularly the side beyond the purifier, as clean as possible.

The cell side of the bellows valve is connected to a tee fitting. One arm of the fitting connects to the transfer reservoir. The probe is a 1/4 by 8 inch stainless steel tube, extending downward and welded shut at the end. By immersing the probe in liquid nitrogen, argon can be drawn from other parts of the system and condensed.

The other side of the tee connects through a metal-to-glass seal to the purifier. The purifier is a 2 cm diameter quartz glass tube filled with zirconium and titanium turnings. The turnings are held in the tube by glass fiber plugs backed by phosphor bronze springs.

Around the tube is a cylindrical electric furnace encased in fire brick insulation. The furnace can heat the turnings to about 1000C. At this temperature the turnings will strongly adsorb oxygen, nitrogen and other electronegative impurities in the argon. Graded glass bands on either side of the purifier protect the rest of the glassware from thermal stress.

Beyond the purifier is the detector. It is a vertical glass cylinder 4 cm in diameter and 25 cm high. The purifier tube enters its side 5 cm from the top. A round-bottomed cylindrical nipple, 1 cm wide by 3 cm high, extends from the bottom of the cylinder. The nipple is silver plated on its interior and the plating extends in a strip up the side of the cylinder to within 4 cm of the top. The silver plating is the detector cathode.

The top of the cylinder is attached to a copper gasket flange with a seven-lead tube feedthrough flange sealing the end. Four of the feedthroughs contain stainless steel rods used as electrical connectors. The FET source, drain, and feedback connections use three of these. The fourth electrical connector is a 5 cm stainless steel rod with a phosphor-bronze spring strip soldered to its end. The spring contacts the silver plating on the side of the cylinder. This is the high voltage biasing lead. The last three feedthroughs contain the legs of the anode probe support. All of the feedthroughs are solder sealed.

The anode probe is a 1 cm diameter glass tube centered in the cylinder and extending its length. It is held in place by the probe support bracket, a stainless steel, Teflon-lined ring clamp attached to three 10 cm legs. The top of the probe is flared and pressed against the center feedthrough in the flange. The bottom of the probe

is sealed to a 1mm molybdenum steel wire. The wire extends to within 0.5cm of the bottom of the nipple and forms the anode. The other end of the wire connects to the FET electronics.

The FET and the feedback electronics are mounted in a cut out section of the probe 5 cm above the end of the probe glass. The gate of the FET and the feedback resistor and capacitor are soldered to a copper ferrule which fits over the top of the anode wire. The ferrule is secured by a set screw. The feedback lead is Teflon insulated wire which runs up the inside of the probe tube to the center feedthrough in the flange. The drain of the FET is connected to a small diameter coaxial cable which leads parallel to the probe up to a flange feedthrough. The source of the FET is connected to the coaxial shield. The other end of the shield leads through another feedthrough to ground. The rest of the preamplifier electronics are connected to the flange feedthroughs by spring connectors. The flange itself is grounded to serve as a guard ring.

Second Detector

The second detector uses the same transfer reservoir as the first detector. A second purifier was constructed to the same design as the first. The end of the purifier tube is connected to 1 cm glass tubing which turns upward and then down to enter the cell chamber through an o-ring seal. The inverted U in the tube provides strain relief for the glassware. The tube goes 15 cm down into the cell chamber, bends about 70 degrees and connects to the cell.

The cell consists of two Kovar metal cups sealed to each end of a glass tube. The bottom cup is 1.3 cm in diameter by 2.5 cm in height. It forms the detector cathode. The top cup is only 2 cm high and is

the guard ring. The center of the top cup is cut out and a tube feedthrough is silver soldered to it. The feedthrough holds a 1/8 inch stainless steel rod 8 cm long. The rod extends to 0.6 cm from the bottom of the lower cup and forms the detector anode. The rod was turned down to 1/16 inch to fit the feedthrough and butted against the feedthrough insulator to minimize vibration. Silver solder seals both ends of the feedthrough.

The cell chamber consists of a brass top cup 6 cm in diameter by 5 cm high connected to a stainless steel bottom cup by an o-ring flange. The bottom cup is 17 cm high. The flange on the bottom cup is a slip ring which allows the cup to be turned to any position before the flange is tightened.

Extending through the bottom of the lower cup is a 3 cm diameter copper bar which acts as a heat pipe. The top of the bar is threaded to a copper tube which contains a cylinder of boron nitride. A well in the top of the boron nitride contains the cathode cup of the detector cell. The boron nitride acts as an electrical insulator and heat conductor. Another small hole in the top of the boron nitride contains an iron-constantan thermocouple. The copper tube surrounding the boron nitride is wrapped with a 40 ohm heater wire. The space between the boron nitride and the copper is filled with high vacuum grease to improve heat conduction. Two tube feedthroughs for the thermocouple and two electrical feedthroughs for the heater are spaced around the top of the lower cup and secured with epoxy.

The top of the brass upper cup has an o-ring seal connector for the cell tube, a 1/2 inch brass tube for a vacuum line and a high voltage Kings connector feedthrough. In the side of the top cup is an

8 lead electrical feedthrough for the preamplifier leads. A clamp and bracket around the upper cup holds the preamplifier.

The FET gate, feedback electronics and test input capacitor are connected to the anode. The test input is through a 1 pf +/-5% capacitor. The drain, source, feedback, and test input are connected to the 8 lead feedthrough with Teflon coated wire. The biasing voltage for the detector enters through the Kings connector, passes through a resistor-capacitor filter network in the upper chamber cup and goes to the cathode cup through a Teflon coated wire.

The bottom of the cell chamber is inserted into a dewar filled with liquid nitrogen. The inside of the chamber is evacuated to provide electrical and thermal insulation. A disk of aluminum foil is hung horizontally on the preamplifier leads just below the flange. It acts as a radiation shield.

Electronics

The electronics used with both detectors consist of a preamplifier, an amplifier, and a multichannel analyzer. An oscilloscope is used to monitor the output of the preamplifier and amplifier. A high voltage power supply provides biasing voltage for the detector. Figure 8 is a diagram of the system electronics.

APPENDIX B

OPERATING PROCEDURES FOR THE CRYOGENIC ARGON DETECTORS

The two argon detectors are operated in much the same way. Only temperature control and the gas purification steps are different. Each stage of operation is described below, with the variations for the different detectors identified. The components and valves are identified in figure 5. The cell chamber valve for the second detector is not shown but is located on the vacuum manifold.

Purging

1. Open the cell valve and GHS valve.
2. Open the argon valve and pressurize the system to about 1000 Pace units (PU).
3. Close the argon valve and open the mechanical pump valve. Pump until the pressure is less than about 10 microns.
4. Close the mechanical pump valve.
5. Repeat 2 through 4 as often as desired.

Cleaning

1. Open all valves except the argon valve, the breakseal valve, the cell chamber valve and the two pump valves.
2. Open the mechanical pump valve. Pump until the pressure is less than about 10 microns.

3. Close the mechanical pump valve and open the ion pump valve. Pump to the desired pressure, ideally about 10^{-7} torr. Heat may be applied to the system but avoid heating the FET, valve seats, o-rings or the swage-lok seals. The purifier should be operating at greater than 700C.

4. Close all valves.

Introducing the Sample

1. Put the sample breakseal bottle on the breakseal connector.

2. Open the breakseal valve, GHS valve and mechanical pump valve. Pump until the pressure is less than about 10 microns.

3. Close the mechanical pump valve and open the ion pump valve. Pump to the desired pressure.

4. Close the ion pump valve and GHS valve and open the cell valve.

5. Cool the transfer reservoir with liquid nitrogen (LN).

6. Break the breakseal tip and wait about 3 minutes.

7. Close the cell valve and breakseal valve.

Introducing the Argon

1. Cool the transfer reservoir with LN.

2. Open the argon valve and pressurize the GHS to about 1000 Pace units (PU).

3. Close the argon valve and open the cell valve. Close the cell valve when the GHS reaches the desired pressure.

4. Repeat 2 and 3 until the sum of the higher pressures minus the sum of the lower pressures equals about 2000 PU (about 1200 for the first detector). If the detector is to be operated with the cell valve open in order to measure pressure, add argon to the GHS until the pressure equals the expected operating pressure (probably about 1000 PU). This

procedure insures that 3 ml of liquid argon will be available for the detector.

Purifying the Argon and Sample (1st Detector)

1. Make sure the purifier is between 700C and 1000C.
2. Cool the detector cell with LN. Allow the transfer reservoir to warm.
3. Cool the transfer reservoir with LN. Allow the detector cell to warm.
4. Repeat 2 and 3 as often as needed to reach the desired purity. Once the desired purity is reached, the process may be stopped at 2.

Purifying the Argon and Sample (2nd Detector)

1. Open the cell chamber valve and mechanical pump valve. Pump until the pressure reaches less than about 10 microns.
2. Close the mechanical pump valve and open the ion pump valve. The ion pump should hold the cell chamber at less than 10^{-5} torr.
3. Open the cell valve.
4. Immerse the bottom of the cell chamber in LN. Cool the detector to -189C.
5. Allow the transfer reservoir to warm very slowly. Keep the cell pressure at or below 1200 PU. Do not allow the pressure within the cell to rise above 1600 PU.
6. Cool the transfer reservoir with LN.
7. Allow the detector cell to warm to about -160C. This can be done by removing the LN or operating the heater.
8. Repeat 4 through 7 as often as needed to reach the desired purity. Once the desired purity is reached, the process may be stopped at 5.

Spectrum Collection

1. Turn on preamplifier, amplifier, high voltage power supply, oscilloscope and multichannel analyzer.
2. Slowly apply negative biasing voltage to the detector while observing the output of the preamplifier on the oscilloscope. If large amplitude pulses (more than a few mV) occur, immediately reduce the biasing voltage. High voltage breakdown occurs at about 1700 V.
3. Adjust the gain of the amplifier while observing the output of the amplifier on the oscilloscope. The observed pulses should be between 1 and 10 V.
4. Set the desired collection time on the multichannel analyzer and begin spectrum collection.

APPENDIX C

THE INTERDIFFUSION OF XENON THROUGH ARGON

The rate of diffusion of one gas through another is found through the use of an interdiffusion coefficient. The interdiffusion coefficient is determined from:

$$D_{12} = \frac{\left(v_1^2 + v_2^2\right)^{\frac{1}{2}}}{3\pi n\, d_{12}^2} \qquad (4:1.186)$$

where D_{12} is the interdiffusion coefficient for gas 1 through gas 2, v is the molecular velocity, n is the molecular density and d_{12} is the average molecular diameter. The molecular velocity can be found from:

$$v = 12{,}895 \left(\frac{T}{m}\right)^{\frac{1}{2}} \qquad (4:1.24)$$

where T is the gas temperature in degrees K, and m is the molecular weight. The average molecular diameter is defined as:

$$d_{12} = \frac{d_1 + d_2}{2}$$

where d_1 is the molecular diameter of gas 1 while d_2 is the molecular diameter of gas 2.

Since both argon and xenon are monatomic gases, the atomic weight and diameter are used. The ideal gas assumption is used to calculate

the atomic density. The following values are used to determine the interdiffusion coefficient of xenon through argon at 200 torr and 295 degrees K:

Atomic weight, Argon	40
Atomic weight, Xenon	133
Atomic Diameter, Argon	3.6 X 10-8 cm (4)
Atomic Diameter, Xenon	4.9 X 10-8 cm (4)
Atomic Density	7.07 X 10 18 atoms/cm^3

These values give an interdiffusion coefficient of 0.32 cm^2/sec.

To estimate the time required for the xenon to diffuse through the system, the following approximations are made. First, all of the xenon is assumed to be at the same distance from the cell; 1 meter. Second, resistance from tube walls, elbows and valves are neglected. Finally, the vapor pressure of the xenon in the cell is assumed negligible. In effect, the xenon is assumed to be diffusing from a plane surface through an infinite volume of argon. The average distance traveled by the xenon atoms diffusing in this manner is found from:

$$Z = 2\left(\frac{D_{12}t}{\pi}\right)^{\frac{1}{2}} \qquad (4:1.199)$$

where Z is the diffusion distance and t is the time. Solving for t gives a value of 6.8 hours. Because resistance is neglected, this is a minimum value.

VITA

Stephen Rolph Berggren was born in Louisville, Kentucky on 7 September, 1949. He received his Bachelor of Science in Chemical Engineering from Rose-Hulman Institute of Technology in June, 1971. He entered the Air Force the same year and was commissioned through the ACP in February, 1974. He was the Reentry Vehicle Maintenance Officer at Whiteman AFB until 1976. He then became the Munitions Services Branch Chief at Anderson AFB until 1977. He then went to Vandenberg AFB and became a Munitions Evaluation Team Chief. In August, 1980 he entered the School of Engineering, Air Force Institute of Technology.

Permanent address: 104 Ridgeway Ave.
Louisville, Kentucky 40207

UNCLASSIFIED

SECURITY CLASSIFICATION OF THIS PAGE (When Data Entered)

REPORT DOCUMENTATION PAGE		READ INSTRUCTIONS BEFORE COMPLETING FORM
1. REPORT NUMBER AFIT/GNE/PH/82-3	2. GOVT ACCESSION NO. AD-A124 736	3. RECIPIENT'S CATALOG NUMBER
4. TITLE (and Subtitle) A CRYOGENIC ARGON IONIZATION CHAMBER DETECTOR FOR ANALYSIS OF RADIOACTIVE NOBLE GASES		5. TYPE OF REPORT & PERIOD COVERED MS Thesis 6. PERFORMING ORG. REPORT NUMBER
7. AUTHOR(s) Stephen R. Berggren Capt USAF		8. CONTRACT OR GRANT NUMBER(s)
9. PERFORMING ORGANIZATION NAME AND ADDRESS Air Force Institute of Technology (AFIT-EN) Wright-Patterson AFB, Ohio 45433		10. PROGRAM ELEMENT, PROJECT, TASK AREA & WORK UNIT NUMBERS
11. CONTROLLING OFFICE NAME AND ADDRESS		12. REPORT DATE March, 1982 13. NUMBER OF PAGES 66
14. MONITORING AGENCY NAME & ADDRESS(if different from Controlling Office)		15. SECURITY CLASS. (of this report) Unclassified 15a. DECLASSIFICATION/DOWNGRADING SCHEDULE

16. DISTRIBUTION STATEMENT (of this Report)

Approved for public release; distribution unlimited

17. DISTRIBUTION STATEMENT (of the abstract entered in Block 20, if different from Report)

18. SUPPLEMENTARY NOTES

Approved for public release: IAW AFR 190-17.
LYNN E. WOLAVER
Dean for Research and Professional Development
Air Force Institute of Technology (AIC)
Wright-Patterson AFB OH 45433

19 JAN 1983

19. KEY WORDS (Continue on reverse side if necessary and identify by block number)

Radiation Detectors
Ionization Chambers
Argon
Xenon

20. ABSTRACT (Continue on reverse side if necessary and identify by block number)

Two ionization chamber detectors, using liquid or solid argon as their medium were designed, constructed and tested as an improved means of analyzing quantitatively xenon 131m and xenon 133. Problems with the first detector, including vibrational noise and inadequate temperature control, limited its use to studies using solid argon. In the second design, many operating problems of the first detector were corrected.

Properties of the detectors were studied using external gamma sources and xenon 131m dispersed inside the detector medium. The xenon sample and argon

DD FORM 1 JAN 73 1473 EDITION OF 1 NOV 65 IS OBSOLETE

UNCLASSIFIED

SECURITY CLASSIFICATION OF THIS PAGE (When Data Entered)

were purified and cryogenically pumped into the detector for spectral analysis. Electric field strengths used were from 100 to 900 kV/m. Both the purity of the argon and bias voltages affected resolution by changing the trapping distance of the electrons in the medium. Lower temperatures increased detection efficiency by condensing more of the sample into the cell.

No clearly recognizable energy peak could be found in spectra from external or internal sources. This is attributed to impurities in the argon medium, to positive ion trapping in the flaws of the crystals and to variation in pulse height with the radial position of interaction in the medium. Detection efficiency for an internal xenon source is less than 10 percent. This is attributed to impurities or to the trapping of the xenon sample outside of the cell. Accurate evaluation of the capabilities of this type of detector cannot be made until the xenon sample can be reliably moved to the detector, the argon purity improved and the design modified to eliminate the position dependence of the signals.